

# Valuation of spread options using the fast Fourier transform under stochastic volatility and jump diffusion models

May 19, 2015

MASTER'S THESIS

LUND UNIVERSITY  
FACULTY OF ENGINEERING

*Author:* Max Andersson  
*Supervisor:* Karl Larsson

## Abstract

Spread options have become very popular in basically every sector of the financial markets, although the pricing of these derivatives still remains a challenge. In this thesis we examine the pricing of spread options using the fast Fourier transform (FFT). We implement a FFT method derived by Hurd and Zhou [10] and investigate the performance of the method under three different market models: the 2-asset geometric Brownian motion framework, a stochastic volatility model and a stochastic volatility model including random jumps in the asset dynamics. The third model is essentially a multivariate extension of Bates model where the jumps are distributed according to a compound Poisson process with log-normally distributed jump sizes. In doing so we successfully extend the work of Hurd and Zhou to include random jumps in the asset dynamics. The choice of models is motivated by the diverse applications of the spread options and its widespread usage in the energy markets.

In addition to showing that the method produces accurate prices at an attractive computational expense, we provide valuable information regarding how to specify the parameters inherent in the method, which is well needed for implementation. Lastly we look at the price sensitivity to the various market parameters which is considered fundamental for the understanding of the model and can have implications for both the calibration problem and trading.

*Keywords:* Derivatives pricing, Spread options, Fast Fourier transform, Stochastic volatility, Jump diffusion

## Acknowledgements

This master's thesis was written at the department of Economics at Lund University during the spring of 2015. It was submitted in fulfillment of the requirements for the degree Master of Science in Industrial Engineering and Management.

I would like to express my gratitude and thanks to my supervisor Karl Larsson at the department of Economics for presenting this fascinating topic to me and for providing valuable feedback and input during the process of this thesis.

In addition, I would like to thank Erik Lindström and Magnus Wiktorsson at the department of Mathematical Statistics for showing continuous support and being a source of inspiration during my master's studies.

Lastly my sincerest gratitude goes to my friends and family for their help and encouragement both on and off campus during my five years at Lund University.

# Contents

<b>1</b>	<b>Introduction</b>	<b>4</b>
<b>2</b>	<b>The Spread Option</b>	<b>5</b>
2.1	The Pricing Problem . . . . .	8
<b>3</b>	<b>FFT Pricing</b>	<b>9</b>
3.1	Fourier Analysis . . . . .	9
3.1.1	The Fast Fourier Transform (FFT) . . . . .	10
3.1.2	The Characteristic Function . . . . .	11
3.2	The FFT Pricing Method . . . . .	11
3.2.1	Choice of Step Size $\eta$ . . . . .	13
3.2.2	Complex Gamma Function . . . . .	14
<b>4</b>	<b>Market Models</b>	<b>14</b>
4.1	Bachelier's Model . . . . .	15
4.2	Geometric Brownian Motion . . . . .	16
4.2.1	Margrabe's Formula . . . . .	17
4.2.2	Analytical Approximations . . . . .	18
4.2.3	Numerical Methods . . . . .	20
4.3	Stochastic Volatility . . . . .	23
4.3.1	Fourier Methods . . . . .	23
4.3.2	Monte Carlo Simulation . . . . .	24
4.4	Stochastic Volatility and Jump Diffusion . . . . .	25
4.4.1	Fourier Methods . . . . .	26
4.4.2	Monte Carlo Simulation . . . . .	26
<b>5</b>	<b>Numerical Results</b>	<b>27</b>
5.1	Geometric Brownian Motion . . . . .	27
5.1.1	Accuracy & Speed . . . . .	28
5.1.2	Sensitivity to the Discretization Parameters . . . . .	30
5.1.3	Sensitivity to the Damping Parameters . . . . .	31
5.2	Stochastic Volatility . . . . .	34
5.2.1	Accuracy & Speed . . . . .	34
5.2.2	Sensitivity to the Discretization Parameters . . . . .	37
5.2.3	Sensitivity to the Damping Parameters . . . . .	38
5.2.4	Price Sensitivity to Market Parameters . . . . .	41
5.3	Stochastic Volatility and Jump Diffusion . . . . .	43
5.3.1	Accuracy & Speed . . . . .	43
5.3.2	Sensitivity to the Discretization Parameters . . . . .	48
5.3.3	Sensitivity to the Damping Parameters . . . . .	49
5.3.4	Price Sensitivity to Market Parameters . . . . .	52
<b>6</b>	<b>Conclusions</b>	<b>56</b>
	<b>References</b>	<b>57</b>

# 1 Introduction

In this thesis we investigate the pricing of spread options. Spread options have become very popular in basically every sector of the financial markets due to their designed ability to mitigate unfavorable movements in several indexes. Traded in the equity, fixed income, commodity and foreign exchange markets this derivative serves a diverse set of applications and has become an important tool in risk management, where it plays a vital role in the hedging of basis-risk. It has also become an attractive tool in real option valuation, where it is applied to asset valuation or the hedging of production exposure, see Trigeorgis [20]. The interest in the spread option can also come from a purely speculative place allowing you to bet on the spread between various indexes, or effectively the correlation. We will discuss the spread option and its applications further in section 2. However, regardless of their popularity and widespread usage, the development of pricing and hedging techniques still get a lot of attention, in both businesses and academic circles.

The reason that the pricing of these options still remains a challenge is the inadequate knowledge of the dynamics of the spread between two correlated stochastic processes. It turns out that the more complexity we add to the model in terms of volatility and correlation structures the less we know about the distribution of the difference between the indexes.

The most naive approach is *Bachelier's model* where the spread is modeled as an arithmetic Brownian motion, in this case the underlying indexes are also arithmetic Brownian motions with a constant correlation. In this framework there is an analytical solution to the price of the spread option. However, the model is clearly unrealistic.

If we instead assume that the two underlying indexes can be modeled as geometric Brownian motions with constant correlation we move on to *Samuelson's model* or the two-asset Black-Scholes model (or simpler the 2-GBM model). Under this framework the spread is the difference between two log-normally distributed random variables, for which an analytical expression of the distribution is not known. This means that we have no analytical solution for the price except for the special case when the strike price  $K = 0$ , in which the price of the spread option is given by *Margrabe's formula*. In the more general case we are referred to either analytical approximations or numerical approaches. Under the 2-GBM model we have a number of proposed analytical approximations, including Bachelier's approximation, Kirk [11], Carmona and Durrleman [3], Deng, Li and Zhou [13] and Alexander and Venkatramanan [21]. The numerical schemes consists of one-dimensional numerical integration, Fourier methods based on the results of Carr and Madan [4], Monte Carlo simulation methods and numerical solutions to the partial differential equations. The analytical methods are often faster than the numerical approaches while the second group is generally more accurate and robust. This is a classic dilemma which has spurred a lot of research trying to find a method that is both fast and accurate.

In a realistic setting the above mentioned market model is oftentimes not

satisfactory. To capture the behavior of the financial markets we often want to include stochastic volatility, stochastic correlation or random jumps. By adding these factors to the model we move away from Gaussianity and the one-dimensional numerical integration technique is no longer available. In addition to this the computational expense for Monte Carlo methods and numerical PDE solvers increases substantially.

In this thesis we implement a pricing method based on the fast Fourier transform derived by Hurd and Zhou [10]. We evaluate the method thoroughly under three different market models: the two-asset Black-Scholes model, a stochastic volatility model and a stochastic volatility model including random jumps in the asset processes, thereby extending the work of Hurd and Zhou. We show that the method produces accurate prices in all models at an attractive computational expense. In addition to this we provide valuable information about how to specify the parameters inherent in the method, which is well needed for implementation. Lastly we look at the price sensitivity to the various market parameters which is deemed fundamental for the understanding of the models and can have implications for both the calibration problem and trading.

In section 2 we start off by discussing the spread option and formally defining the pricing problem. Next, in section 3 we review the fast Fourier transform method proposed by Hurd and Zhou and in section 4 we introduce the market models and the pricing algorithms we are considering in each framework. In section 5 we provide the numerical results of the thesis; we evaluate the accuracy and the speed of the method, we analyze the sensitivity to the parameters needed to be specified in the method and we look at the price sensitivity to the various market parameters. Lastly in section 6 we provide a conclusion based on the results.

## 2 The Spread Option

The term spread refers to the difference between two indexes, typically the spread between two rates of returns, the spread between a risky bond and a Treasury bond, or two swap rates. The most natural case for defining a spread option is when the option is written on the difference between the values of two indexes. However, the spread option is extended to include all options written on a linear combination of a finite set of underlying indexes. Referring to the survey performed by Carmona and Durrleman [3] for a more elaborate discussion of the applications of spread options, we will reiterate some of the features of these derivatives and their role as both hedging tools and speculative instruments below.

**Fixed Income Market** In the fixed income market the option is typically written on the spread between two yields. The most traded instruments in the US market are spread options on either different maturities or different quality

levels. An example of the first group being the Note against Bond Spread, the NOB spread, which is an option written on the spread between the prices of Treasury notes and Treasury bonds. In the second group we have the TED spread, which derives its value from the difference in the rates of Treasury bills and Eurodollar bills. Another example in the fixed income market is the spread on the difference between LIBOR rates with different maturities considered by Suárez-Taboada and Vázquez [19]. The payoff of this contract can be written as:

$$(\alpha L_2(T_2) - \beta L_1(T_1) - K)^+$$

where  $L_1$  and  $L_2$  are forward rates fixed at different times  $T_1$  and  $T_2$ ,  $\alpha$  and  $\beta$  some positive constants,  $K$  is the strike price and the notation  $x^+ = \max(x, 0)$ .

**Foreign Exchange Market** In the foreign exchange market spread options are usually based on interest rates in different countries. Examples being the French-German and the Dutch-German bond spreads. A typical example is the cross-currency spread option which, at time to maturity  $T$  and in currency 1, has the payoff:

$$(\alpha Y_1(T) - \beta Y_2(T) - K)^+$$

where the underlying indexes  $Y_1$  and  $Y_2$  are swap rates in possibly different currencies,  $\alpha$  and  $\beta$  positive constants and  $K$  the strike price.

**Commodity Markets** Again referring to Carmona and Durrleman [3] we will highlight some of the applications of spread options in the commodity markets mentioned in their survey. In this market we distinguish between four kinds of spread options:

- *Location spreads* - The associated spread refers to the difference between the prices of a commodity at two different locations.
- *Calendar spreads* - The difference is between the prices of a commodity at two different points in time.
- *Quality spreads* - The spread is the difference between the prices of two quality levels of the same commodity.
- *Processing spreads* - The spread is the difference between the price of the input and the price of the output of a production process.

We provide some classic examples of traded spread options in the commodity markets below.

**The Crush Spread** The *crush spread* consists of the prices of soybean meal and soybean oil, and a futures contract of soybean, thereby relating the price of soybeans to the market price of soybean derivative products. The price of this contract gives the market a quantified hint of the (average) gross processing margin of soybean products. Let us say that on average one “bushel” of soybean gives 48 pounds of soybean meal and 11 pounds of soybean oil when crushed, then the value of the of the crush spread at time  $t$   $[CS]_t$  is given by:

$$[CS]_t = 48[SM]_t/2000 + 11[SO]_t/1000 - [S]_t$$

where  $[S]_t$  is the futures price at time  $t$  of a soybean contract in dollars per bushel,  $[SO]_t$  is the futures price at time  $t$  of a soybean oil contract in dollars per 100 pounds and  $[SM]_t$  is the price of a futures contract at time  $t$  in dollars per ton of soybean meal.

If we now consider the strike price  $K$  to represent the crushing cost it is profitable to crush soybeans when  $[CS]_t - K > 0$ . This spread option is used as a hedging tool by processors or for speculation purposes.

**Crack Spreads** In the energy market a frequently traded spread option is the *crack spread*. This spread also represents a refining margin, but in this case between crude oil and petroleum products. We give examples of two of the most liquid spread options below.

- The 3:2:1 crack spread is made up of three contracts of crude oil, two of unleaded gasoline and one contract of heating oil. This spread can be formulated mathematically as:

$$[CS]_t = \frac{2}{3}[UG]_t + \frac{1}{3}[HO]_t - [CO]_t$$

where  $[UG]_t$  is the futures price at time  $t$  of unleaded gasoline,  $[HO]_t$  is the futures price at time  $t$  of heating oil and  $[CO]_t$  is the futures price at time  $t$  of crude oil.

- The 1:1:0 gasoline crack spread consists of one contract of crude oil and one contract of unleaded gasoline. The spread  $[GCS]_t$  is given by:

$$[GCS]_t = [UG]_t - [CO]_t$$

**Spark Spreads** Another frequently traded spread option in the energy markets is the *spark spread*. The spark spread can be defined as the difference of the price of electricity and the price of the fuel used to generate it and can therefore be used to approximate the cost of converting a fuel into electricity. One of the most liquid contracts is the 4:3 spark spread, represented by the difference between four electricity contracts and three natural gas contracts. We formulate this spread mathematically as:

$$[SS]_t = 4[E]_t - 3[NG]_t$$

However, as Carmona and Durrleman [3] points out, one of the most interesting spread options is on the following form:

$$Spr_t = F_E(t) - H_{eff}F_{NG}(t)$$

where  $F_E(t)$  is the price of a futures contract on electricity,  $F_{NG}(t)$  the price of a futures contract on natural gas and  $H_{eff}$  represents the heat rate, or the efficiency factor of a power plant. Using this formulation we can interpret the spread  $Spr_t$  as the economic value of producing electricity at a specific plant with efficiency factor  $H_{eff}$ . This illustrates why spread options have become popular in real asset valuation. A sum of spark spread options can be used to estimate the operating value of a power plant. Furthermore, a plant owner can use the market information for production planning; when the heat rate coefficient  $H_{eff}$  implied by the spot prices of electric power and gas is above the operating heat rate of the plant, the owner should buy gas, produce electricity and sell it for profit. Similarly, in the opposite case the plant owner is better off shutting down its operation.

We have seen that spread options can be used to quantify the costs of production in the energy markets. Two other short examples from the trading world follows. A trader can use spread options to take advantage of the difference in the price of a commodity at different times in the future. Secondly a trader can hedge risks associated with transportation (or transmissions) by considering futures contracts on the same commodity with physical deliveries at different locations.

In this subsection we have tried to illustrate the diverse nature of the spread option and its many applications in different sectors of the financial markets. In the next subsection we review the mathematical formulation of the spread option pricing problem.

## 2.1 The Pricing Problem

We will for the remainder of this thesis consider the case where the payoff of the spread option is given by the difference of two underlying indexes. The aim will be to price a European option on the underlying spread. As in the vanilla case this option will be defined by a time to maturity  $T$  and a positive number  $K$  representing the strike price, and it will give the holder of the derivative contract the right to purchase one unit of the underlying asset at the price  $K$  at time  $T$ . If we let the stochastic time series  $S_1 = \{S_1(t)\}_{0 \leq t \leq T}$  and  $S_2 = \{S_2(t)\}_{0 \leq t \leq T}$  represent the values of the two underlying indexes, the payoff of a (European) call spread option with strike price  $K$  at time  $t$  is then given by:

$$(S_2(t) - S_1(t) - K)^+$$



where we use the notation  $x^+ = \max(x, 0)$ . Next we consider the two processes to be stochastically defined on some probability space  $(\Omega, \mathcal{F}, \{\mathcal{F}_t\}_{t \geq 0}, \mathbf{P})$ , where  $\mathbf{P}$  is the physical, or historical, measure and  $\{\mathcal{F}_t\}$  is the filtration, which is interpreted as the information collected as time evolves. Furthermore, the processes representing the underlying indexes, are assumed to be adapted to this filtration. Now, according to martingale pricing theory, the price  $p$  of the spread option at time  $t$  is given by an expectation taken under the risk-neutral equivalent measure  $\mathbf{Q}$ :

$$p(S_1(t), S_2(t), K, T) = e^{-r(T-t)} \mathbb{E}_{\mathbf{Q}}((S_2(T) - S_1(T) - K)^+ | \mathcal{F}_t) \quad (1)$$

where  $e^{-r(T-t)}$  is the discounting factor and  $r$  generally is said to be the short rate of interest. However,  $r$  can be defined to include corrections to the discounting factor such as dividend payments or convenience yields. For more background the mathematics behind the continuous arbitrage pricing the reader is referred to the book Björk [2].

### 3 FFT Pricing

In this section we review the fast Fourier transform pricing method that will be implemented in this thesis. However, before we outline the pricing method we will provide some theoretical background, which is considered necessary in order to fully understand the pricing technique. In subsection 3.1 we give a brief introduction to Fourier analysis. We introduce the Fourier transform, the fast Fourier transform algorithm and the characteristic function of a random variable. Next in subsection 3.2 we see how these tools allow us to develop a method to numerically price spread options.

#### 3.1 Fourier Analysis

Since its discovery Fourier analysis has had vast implications for mathematics, science and engineering. Fourier analysis studies how general mathematical functions can be described by sums of trigonometric functions. The study was born from the studies on Fourier series, which is a way to represent a periodic signal by decomposing it into a sum of oscillating sine and cosine functions. The technique was first introduced through the work of the french mathematician Joseph Fourier, who applied Fourier series in his studies of heat transfer originally published in 1807.

While the use of Fourier series lets us rewrite periodic functions into a sum of sinusoidal functions, the Fourier transform is an extension to this and constitutes a powerful tool that allows us to represent a general function as a sum of sinusoids. Remembering that by the use of Euler's formula the trigonometric functions can be rewritten as complex exponential functions of different frequencies we can give the following definition of the Fourier transform:

$$F(\omega) = \mathcal{F}(f(t)) = \int_{-\infty}^{\infty} f(t)e^{-i\omega t} dt \quad (2)$$

$$f(t) = \mathcal{F}^{-1}(F(\omega)) = \frac{1}{2\pi} \int_{-\infty}^{\infty} F(\omega)e^{i\omega t} d\omega \quad (3)$$

where  $f : \mathbb{R} \rightarrow \mathbb{C}$  is an integrable function. The function  $F(\omega)$  in equation 2 is called the Fourier transformation, the Fourier representation or the frequency representation of the original function  $f(t)$ . We see that the Fourier transform is a complex valued function of the frequency, and that the transformation effectively lets us take a function of time and “transform” it into the underlying frequencies that characterizes it. The function  $f(t)$  can be obtained by applying the inverse Fourier transform, equation 3, which essentially combines all of the different underlying frequencies to retrieve the original function. The functions  $f(t)$  and  $F(\omega)$  are representations of the same underlying identity and are sometimes referred to as a Fourier pair. The domain of the complex valued function is often referred to as the frequency domain, or the complex domain, while the domain of the original signal is called the time domain or the real domain. For more background on Fourier analysis see Osgood [17].

### 3.1.1 The Fast Fourier Transform (FFT)

The discrete Fourier transform (DFT) is the discrete version of the (continuous) Fourier transform for a finite data sample. The DFT can be seen as the Fourier transform evaluated for functions only known at  $N$  discrete points separated by some sample time. This is necessary in practice in order to allow for computational methods to be used for evaluating the Fourier transform. The DFT is defined by the following formula:

$$X_k = \sum_{n=0}^{N-1} x_n e^{-i2\pi k \frac{kn}{N}}, k = 0, 1, \dots, N - 1$$

Similarly the inverse DFT is given by:

$$x_k = \frac{1}{N} \sum_{n=0}^{N-1} X_n e^{i2\pi k \frac{kn}{N}}, k = 0, 1, \dots, N - 1$$

The fast Fourier transform (FFT) is an algorithm designed to efficiently compute the discrete Fourier transform by minimizing the number of multiplications and summations. The development of FFT algorithms made the calculation of the DFT practical in many scientific applications due to its large impact on computational time. Evaluating the DFT by simply using the definition takes  $N^2$  multiplications and  $(N - 1)$  additions, that is a computational complexity

of  $O(N^2)$  operations. If we instead apply the FFT, the same DFT can be computed using  $O(N \log N)$  operations, which is fundamental for the use of Fourier methods today. The most widely used FFT algorithm today is the Cooley-Tukey algorithm popularized by Cooley and Tukey [5]. This is a D&C (divide and conquer) algorithm that divides a DFT of size  $N = N_1 N_2$  into smaller DFT's of size  $N_1$  and  $N_2$  recursively. Due to the nature of the algorithm it is the fastest when  $N$  is a power of two  $N = 2^n$ .

### 3.1.2 The Characteristic Function

The characteristic function of a random variable  $X$  with probability density function  $f(x)$  can be defined in the following way:

$$\Phi_t = \mathbb{E}[e^{itX}] = \int_{-\infty}^{\infty} e^{itx} f(x) dx$$

We note that the characteristic function of  $X$  is essentially the inverse Fourier transformation of its probability density function  $f$ , except for a scaling factor of  $2\pi$ . Since the characteristic function completely determines the probability distribution of  $X$  this opens up a new approach to many problems, including option pricing. In the next subsection we see how we can develop a numerical pricing method for spread options using the FFT based on the knowledge of a joint characteristic function of the return process.

## 3.2 The FFT Pricing Method

Pricing methods based on the Fourier transform use the characteristic function of the log-price process to retrieve an expression of the price that can be approximated using the fast Fourier transform (FFT) (or some other transform method). These methods have become widely used since their introduction by Carr and Madan [4] due to their accuracy and speed. However, they have introduced some numerical challenges. In 2009 Hurd and Zhou [10] developed a new FFT implementation that extends the method of Carr and Madan to a multivariate setting. In their paper, Hurd and Zhou introduces a new approach to numerically price spread options in two dimensions (or higher), through an innovative implementation of the FFT. Their approach can be applied as long as the characteristic function of the joint return process is given analytically. A summary of Hurd and Zhou's FFT method is provided below.

The method has its starting point in the following mathematical result: Consider the payoff function of a spread option with strike price  $K = 1$  given by  $P(x_1, x_2) = (e^{x_1} - e^{x_2} - 1)^+$ . The Fourier representation of  $P(x_1, x_2)$  is then given by:

*Theorem 1: For any real numbers  $\epsilon = (\epsilon_1, \epsilon_2)$  with  $\epsilon_2 > 0$  and  $\epsilon_1 + \epsilon_2 < -1$*

$$P(x) = (2\pi)^{-2} \int \int_{\mathbb{R}^2 + i\epsilon} e^{iux'} \hat{P}(u) d^2u, \hat{P}(u) = \frac{\Gamma(i(u_1 + u_2) - 1) \Gamma(-iu_2)}{\Gamma(iu_1 + 1)} \quad (4)$$

Here  $\Gamma(z)$  is the complex gamma function defined for  $\Re(z) > 0$  by the integral  $\Gamma(z) = \int_0^\infty e^{-t} t^{z-1} dt$ . We write  $u = (u_1, u_2)$  and  $x = (x_1, x_2)$  and the notation  $x'$  denotes the (unconjugated) matrix transpose.

The damping coefficients  $\epsilon = (\epsilon_1, \epsilon_2)$  are introduced in order to achieve a square-integrable Fourier representation of the spread option payoff. Given this result we can combine equation (4) with the characteristic function of the bivariate stochastic variable  $X(t) = (\log S_1(t), \log S_2(t))$  to compute the spread option price given by equation (1). If we make the assumption that for any  $t > 0$  the increment  $X_t - X_0$  is independent of  $X_0$ , the characteristic function of  $X(T)$  can be factorized in the following way:

$$\mathbb{E}_{\mathbb{Q}}[e^{iuX'_T} | X_0] = e^{iuX'_0} \Phi_T(u), \text{ where } \Phi_T(u) \equiv \mathbb{E}_{\mathbb{Q}}[e^{iuX'_T}]$$

In this setting  $\Phi_T(u)$  is independent of the initial vector  $X_0$ . This assumption holds true for most typical market models, and implies that the price of a spread option with time to maturity  $T$  and strike price  $K = 1$  is given by:

$$\begin{aligned} p &= e^{-rT} \mathbb{E}_{\mathbb{Q}}[(S_2(T) - S_1(T) - 1)^+] = (2\pi)^{-2} e^{-rT} \int \int_{\mathbb{R}^2 + i\epsilon} \mathbb{E}_{\mathbb{Q}}[e^{iuX'_T} | X_0] \hat{P}(u) d^2u \\ &= (2\pi)^{-2} e^{-rT} \int \int_{\mathbb{R}^2 + i\epsilon} e^{iuX'_0} \Phi_T(u) \hat{P}(u) d^2u \end{aligned} \quad (5)$$

where the vector  $S(t) = e^{-Xt}$ .

The price given by equation (5) is a double Fourier integral and can be approximated by a two-dimensional FFT. To approximate the integral by a double sum we need to discretize both the complex and the real domain, which is done by Hurd and Zhou in the following way:

$$\Gamma = \{u(k) = (u(k_1), u(k_2)) | k = (k_1, k_2) \in \{0, \dots, N-1\}^2, u(k) = -\bar{u} + k\eta\}$$

$\Gamma$  defines the complex grid and is specified by our choices of number of discretization points  $N$  (should be a power of 2) and the grid spacing  $\eta$ . Given our choices of  $N$  and  $\eta$  we have in turn specified the truncation error on the integration interval  $[-\bar{u}, \bar{u}]$ . Now we can discretize the real domain as:

$$\begin{aligned} \Gamma^* &= \{x(l) = (x(l_1), x(l_2)) | l = (l_1, l_2) \in \{0, \dots, N-1\}^2, \\ &x(l) = -\bar{x} + l\eta^*, \bar{x} = N\eta^*/2 \end{aligned}$$

where  $\eta^* = 2\pi/(N\eta) = \pi/\bar{u}$ .

For an initial price vector  $S_0 = e^{X_0}$ , with  $X_0$  on the real grid, that is  $X_0 = x(l) \in \Gamma^*$ , we now have the following approximation of the spread option price (with time to maturity  $T$  and strike price  $K = 1$ ):

$$p(S_0) \approx \frac{\eta^2 e^{-rT}}{(2\pi)^2} \sum_{k_1, k_2=0}^{N-1} e^{i(u(k)+i\epsilon)x(l)'} \Phi_T(u(k) + i\epsilon) \hat{P}(u(k) + i\epsilon) \quad (6)$$

Utilizing the double inverse discrete Fourier transform we can rewrite equation (6) as:

$$\begin{aligned} p(S_0) &\approx (-1)^{l_1+l_2} e^{-rT} \left( \frac{\eta N}{2\pi} \right)^2 e^{-\epsilon x(l)'} \left[ \frac{1}{N^2} \sum_{k_1, k_2=0}^{N-1} e^{2\pi i k l' / N} H(k) \right] \\ &= (-1)^{l_1+l_2} e^{-rT} \left( \frac{\eta N}{2\pi} \right)^2 e^{-\epsilon x(l)'} [i f f t 2(H)](l) \end{aligned} \quad (7)$$

where

$$H(k) = (-1)^{k_1+k_2} \Phi_T(u(k) + i\epsilon) \hat{P}(u(k) + i\epsilon) \quad (8)$$

and  $\hat{P}$  is the Fourier transform of the payoff function for the spread option defined in equation (4),  $\Phi$  is the characteristic function of the market model and  $i f f t 2(H)$  is the 2-dimensional inverse FFT of the matrix  $H$ .

Remember that equation (7) yields the price of a spread option with strike price  $K = 1$ . However, this is without loss of generality since we can extend it to the general case ( $K > 0$ ) by a simple scaling of  $S_1$  and  $S_2$ . The pricing formula can then be rewritten as:

$$p(S_2(0), S_1(0), K, T) = K \cdot p\left(\frac{S_2(0)}{K}, \frac{S_1(0)}{K}, 1, T\right)$$

### 3.2.1 Choice of Step Size $\eta$

The FFT method requires that we specify the number of discretization points  $N$  and the step size in the complex domain  $\eta$  which in turn decides the step size in the real plane  $\eta^* = 2\pi/N\eta$ . The original method uses equal step sizes for both axis in the two domains. However, in this thesis we will instead apply an algorithm suggested by Olivares and Cane [16]. See algorithm 1 below (where a typo in the original article has been corrected). By letting the step size vary along each axes of each plane this algorithm lets us find a step size chosen in such a way that each initial asset price is on the grid (no need for interpolation

between grid points) with a maximum truncation error, specified by a minimum integration interval in the complex plane  $\bar{u}_{min}$ .

---

**Algorithm 1** Algorithm for choosing step size  $\eta_m$  given  $N$  and  $\bar{u}_{min}$ .

---

1. Select  $N$  and  $\bar{u}_{min}$
  2. For each asset  $m = 1, 2$ , with initial price  $S_m(0)$  set the log-price  $X_m(0) = \log S_m(0)/K$ . Where  $K$  is the strike price.
  3. Set  $\bar{u}_{test} = \frac{\pi(i-N/2)}{X_m(0)}$
  4. If  $\bar{u}_{test} > \bar{u}_{min}$  return  $\bar{u}_{test}$
  5. Else loop
- 

### 3.2.2 Complex Gamma Function

Implementation of the method requires calculation of the complex Gamma function in equation (4). In this thesis we use a complex Gamma function written by Godfrey [8], which is based on an implementation of the Lanczos approximation. This function is valid in the entire complex plane and supposedly accurate up to 15 significant digits in the real axis and up to 13 significant digits otherwise.

## 4 Market Models

As stated in the introduction we will price spread options under three different market models. Although, first Bachelier's model is reviewed, which in practice is an approximation to the first of the other three models. The first market model we consider is the classic Samuelson's model, where the underlying indexes are modeled as two geometric Brownian motions with a constant correlation. This model is discussed in subsection 4.2 below where we formally define the model and review some of the pricing methods that are available under this framework. In the following subsection we extend the first model to include stochastic volatility. This is done by introducing a stochastic process representing the volatility and in turn letting the volatility of the underlying indexes depend on this process. The resulting model is essentially a multivariate extension of the Heston model introduced by Steven Heston [9]. Lastly, we further extend the model to include independent jumps in the asset dynamics. The jump sizes will be log-normally distributed and arrive according to a Poisson process. Analogous to the Heston case this will be a multivariate extension of Bates [1].

These models allow us to describe certain well-known behaviors of the financial markets and therefore to calibrate our model to better reflect the true dynamics of the complex reality. For example, it is widely considered that stochastic volatility is a necessary characteristic in the equities market, and to explain volatility smiles. Furthermore, random jumps are often needed to capture price spikes in the commodity markets. This motivates our choice of models since spread options are popular as a hedging tool in the energy markets. In

conclusion, pricing spread options under jump diffusion models is relevant for risk management and trading, as well as for real option and asset valuation.

#### 4.1 Bachelier's Model

For reasons of completeness we will consider Bachelier's model before we venture into Samuelson's model below. In the Bachelier model we do not model the underlying indexes individually, instead the spread itself is modeled. The rationale behind this is that studies seem to suggest that the distribution of the spread looks like a normal distribution. This observation proposes that the spread dynamics can be modeled as a single arithmetic Brownian motion. That is, the spread  $Spr(t) = S_2(t) - S_1(t)$  has dynamics of the form:

$$dSpr(t) = \mu Spr(t)dt + \sigma d\mathbf{W}(t)$$

where  $\mu$  and  $\sigma$  are positive constants and  $\mathbf{W}(t)$  is a Wiener process. Under this assumption it is possible to derive a closed form analytical expression (à la Black-Scholes) for the spread option price. If the value of the spread is assumed to have a normal distribution the price of a spread option with strike price  $K$  and time to maturity  $T$  is given by:

$$p = (m(T) - Ke^{-rT})N\left(\frac{m(T) - Ke^{-rT}}{s(T)}\right) + s(T)n\left(\frac{m(T) - Ke^{-rT}}{s(T)}\right)$$

where  $n()$  and  $N()$  are the standard Gaussian density function and the cumulative Gaussian distribution respectively and

$$m(T) = (S_2(0) - S_1(0))e^{(\mu-r)T}$$

$$s^2(T) = e^{2(\mu-r)T} \left( S_1(0)^2 \left( e^{\sigma_1^2 T} - 1 \right) - 2S_1(0)S_2(0)(e^{\rho\sigma_1\sigma_2 T} - 1) + S_2(0)^2(e^{\sigma_2^2 T} - 1) \right)$$

where  $r$  is the short rate,  $\mu$  is the short rate  $r$  minus some continuous dividend rate or convenience yield,  $\sigma_i$  denotes the volatility of asset  $i$  respectively and  $\rho$  the correlation between the underlying indexes.

Note that the assumption of the spread being Gaussian implies that the underlying indexes can also be modeled as arithmetic brownian motions, which of course is unrealistic since they can be negative. What people do in practice however is that they assume that the indexes  $S_1$  and  $S_2$  follow geometric Brownian motions while keeping the assumption that the spread is Gaussian. This is a direct contradiction but the motivation is the fact that empirical studies seem to show that the distribution of the difference between two random variables with log-normal distributions looks almost like a normal distribution, see Carmona and Durrleman [3].

## 4.2 Geometric Brownian Motion

In this part we move on to model the two underlying indexes individually. Now we consider the case where the risk-neutral dynamics of the underlying indexes are given by correlated geometric Brownian motions. This is the framework where most of the earlier previous work on spread options have been focused. The model is often referred to as the 2-asset Black-Scholes model, the 2-factor GBM model, or Samuelson's model. Paul Samuelson was the first one to introduce the geometric Brownian motion as the underlying stock price process in his 1965 pricing model, which now has become the standard stochastic process for stock returns and lead to the widely used Black-Scholes formula. For a more thorough review of the influence of Paul Samuelson on financial economics, see Merton [15].

In this model the distribution of the spread is given by the difference of two log-normally distributed variables. Unfortunately, this means that the price of the spread option can not be expressed by a formula in closed form. An exception is when the strike price  $K = 0$  in which case the price is given analytically by Margrabe's formula, which was derived by William Margrabe [14]. In the 2-GBM framework the risk neutral dynamics of the underlying processes are given by:

$$dS_1 = S_1(r - \delta_1)dt + \sigma_1 S_1 d\mathbf{W}_1$$

$$dS_2 = S_2(r - \delta_2)dt + \sigma_2 S_2 d\mathbf{W}_2$$

where  $r$  is the risk free rate,  $\delta_i, \sigma_i$  denotes the continuous dividend rate and the volatility of asset  $i$  respectively and  $\mathbf{W}_1$  and  $\mathbf{W}_2$  are two Wiener processes with correlation  $\rho$ . If we instead consider the log-prices and apply Ito's formula we have the dynamics:

$$d\log S_1 = (r - \delta_1 - \frac{1}{2}\sigma_1^2)dt + \sigma_1 d\mathbf{W}_1$$

$$d\log S_2 = (r - \delta_2 - \frac{1}{2}\sigma_2^2)dt + \sigma_2 d\mathbf{W}_2$$

Since we are focusing on European options in this thesis we only need to consider the distribution of the spread at time  $T$ . With this in mind and the dynamics given by the stochastic differential equations above we can rewrite the pricing formula equation (1) at time  $t = 0$  as:

$$p = e^{-rT} \mathbb{E}_{\mathbb{Q}} \left\{ \left( s_2 e^{(r-\delta_2-\frac{1}{2}\sigma_2^2)T+\sigma_2 W_2(T)} - s_1 e^{(r-\delta_1-\frac{1}{2}\sigma_1^2)T+\sigma_1 W_1(T)} - K \right)^+ \right\} \quad (9)$$

where the initial conditions are  $S_2(0) = s_2$  and  $S_1(0) = s_1$ .



#### 4.2.1 Margrabe's Formula

As previously mentioned the only case where we have an explicit solution for the spread option price in the 2-GBM framework is when the strike price  $K = 0$ . In this case the price is given by Margrabe's formula which was first derived by William Margrabe in 1978. The price of a spread option with strike price  $K = 0$  and time to maturity  $T$  is given by:

$$p = s_2 e^{-\delta_2 T} N(d_2) - s_1 e^{-\delta_1 T} N(d_1)$$

where  $N()$  is the cumulative normal distribution and:

$$d_2 = \frac{\log(s_2/s_1) - (\delta_2 - \delta_1)T}{\sigma\sqrt{T}} + \frac{1}{2}\sigma\sqrt{T}$$

$$d_1 = \frac{\log(s_2/s_1) - (\delta_2 - \delta_1)T}{\sigma\sqrt{T}} - \frac{1}{2}\sigma\sqrt{T}$$

and:

$$s_2 = S_2(0), s_1 = S_1(0)$$

$$\sigma = \sqrt{\sigma_1^2 + \sigma_2^2 - 2\rho\sigma_1\sigma_2}$$

For the proof the reader is referred to Margrabe [14].

It is worth mentioning that the case  $K = 0$  is not irrelevant, it corresponds to the option to exchange one asset for another. This is illustrated well in Carmona and Durrleman [3] where the authors provide the following argument: Let us assume that our business requires the purchase of one of two products at time  $T$ . From a business perspective it does not matter which one, but the decision has to be made at time  $t$ . Let us then purchase asset 2 and at the same time the zero strike spread option. If the product we bought ends up being cheaper at time  $T$  we choose not to exercise the option, thus wasting the premium. But in the other case, if the asset we chose ends up being more expensive than the other product at time  $T$ , we receive the price difference by exercising the option. In conclusion, the spread option guarantees that we will do as well regardless of what product we choose at time  $t$ . Thus, covering the premium at time  $t$  provides a hedge against unfavorable market moves.

However, when  $K \neq 0$  no closed form solution is available since the expectation in the pricing equation (9) cannot be evaluated analytically and we are therefore referred to approximations. Extensive research have been carried out in order to find both analytical approximations and numerical schemes to price the option and calculate the sensitivities, see the next section.

### 4.2.2 Analytical Approximations

**Kirk's Approximation** Ever since Kirk proposed an approximate price formula for a European call spread option in 1995, Kirk's approximation has become extensively used among the practitioners. The approximation was first published by Kirk [11] in 1995 and provides a Black-Scholes-like formula that is valid for small strike prices  $K$ . A derivation of the formula is given in Venkatramanan and Alexander [21] where the authors use that when  $K \ll S_1(t)$ ,  $S_1(t) + K$  can be assumed to be approximately log-normal, which implies that the ratio between  $S_2(t)$  and  $S_1(t) + Ke^{-r(T-t)}$  can be expressed as a geometric Brownian motion. Following their procedure, defining the processes  $Z(t) = \frac{S_2(t)}{Y(t)}$  and  $Y(t) = S_1(t) + Ke^{-r(T-t)}$  the price of the spread option at time  $t$  is given by:

$$p(t) = S_2(t)e^{-\delta_2(T-t)}N(d_{1Z}) - (Ke^{-r(T-t)} + S_1(t))e^{-(r-(\tilde{r}-\tilde{\delta}_1))(T-t)}N(d_{2Z}) \quad (10)$$

where  $N(\cdot)$  is the cumulative normal distribution and:

$$d_{1Z} = \frac{\log(Z) + (r - \delta_2 - (\tilde{r} - \delta_1) + \frac{1}{2}\sigma^2)(T - t)}{\sigma(T - t)}$$

$$d_{2Z} = d_{1Z} - \sigma\sqrt{T - t}$$

$$\tilde{\sigma}_1 = \sigma_1 \frac{S_1(t)}{Y(t)}$$

$$\tilde{r} = r \frac{S_1(t)}{Y(t)}$$

$$\tilde{\delta}_1 = \delta_1 \frac{S_1(t)}{Y(t)}$$

$$\sigma = \sqrt{\tilde{\sigma}_1^2 + \sigma_2^2 - 2\rho\tilde{\sigma}_1\sigma_2}$$

**Deng, Li, Zhou Approximation** In their paper that was published 2008 Deng, Li and Zhou [13] develop a new closed-form approximation for spread options. A summary of their method is provided below.

The authors start off by noting that  $\log S_1(T)$  and  $\log S_2(T)$  are jointly Gaussian distributed with means  $\mathbb{E}_{\mathbb{Q}}[\log S_i(T)] = \mu_i$  and variances  $\mathbb{V}_{\mathbb{Q}}[\log S_i(T)] = v_i^2$  given by:

$$\mu_i = \log S_i + (r - \delta_i - \frac{1}{2}\sigma_i^2)T$$

$$v_i = \sigma_i\sqrt{T}$$

By defining the standardized log prices as:

$$X = \frac{\log S_2(T) - \mu_2}{v_2}, Y = \frac{\log S_1(T) - \mu_1}{v_1}$$

we see that, since the options are in-the-money if  $S_2(T) - S_1(T) - K \geq 0$ , this is equivalent to the condition below:

$$X \geq \frac{\log(e^{v_1 Y + \mu_1} + K) - \mu_2}{v_2}$$

Therefore, conditioning on  $Y = y$ , the option is in-the-money if  $X \geq \underline{x}(y)$ . We denote  $\underline{x}(y)$  as the exercise boundary and define it as:

$$\underline{x}(y) \equiv \frac{\log(e^{v_1 y + \mu_1} + K) - \mu_2}{v_2}$$

The authors now state that the price of the spread option is given by:

$$p = e^{v_2^2/2 + \mu_2 - rT} \mathbf{I}_1 - e^{v_1^2/2 + \mu_1 - rT} \mathbf{I}_2 - K e^{-rT} \mathbf{I}_3 \quad (11)$$

where the  $\mathbf{I}_i$ 's are given by:

$$\mathbf{I}_1 = \int_{-\infty}^{\infty} N(A(y + \rho v_2) + \sqrt{1 - \rho^2} v_2) n(y) dy$$

$$\mathbf{I}_2 = \int_{-\infty}^{\infty} N(A(y + v_1)) n(y) dy$$

$$\mathbf{I}_3 = \int_{-\infty}^{\infty} N(A(y)) n(y) dy$$

where  $n()$  and  $N()$  are the standard Gaussian density function and the cumulative Gaussian distribution and the function  $A()$  is given by:

$$A(y) = \frac{\rho y - \underline{x}(y)}{\sqrt{1 - \rho^2}}$$

In order to achieve a closed-form approximation of the price Deng, Li and Zhou [13] approximate the integrals  $\mathbf{I}_i$ , which is based on a quadratic approximation of the function  $A()$ , in the following way:

$$\mathbf{I}_i \approx \mathbf{J}_0(C^i, D^i) + \mathbf{J}_1(C^i, D^i)\epsilon + \frac{1}{2}\mathbf{J}_2(C^i, D^i)\epsilon^2$$

where the  $\mathbf{J}_i$ -functions are defined as:

$$\begin{aligned}\mathbf{J}_0(u, v) &= N\left(\frac{u}{\sqrt{1+v^2}}\right) \\ \mathbf{J}_1(u, v) &= \frac{1 + (1+u^2)v^2}{(1+v^2)^{5/2}} \cdot n\left(\frac{u}{\sqrt{1+v^2}}\right) \\ \mathbf{J}_2(u, v) &= \frac{(6-6u^2)v^2 + (21-2u^2-u^4)v^4 + 4(3+u^2)v^6 - 3}{(1+v^2)^{11/2}} u \cdot n\left(\frac{u}{\sqrt{1+v^2}}\right)\end{aligned}$$

Lastly the arguments  $C^i$  and  $D^i$ , and  $\epsilon$  are given by:

$$\begin{aligned}C^1 &= C^3 + D^3 \rho v_2 + \epsilon \rho^2 v_2^2 + \sqrt{1-\rho^2} v_2 \\ D^1 &= D^3 + 2\rho v_2 \epsilon \\ C^2 &= C^3 + D^3 v_1 + \epsilon v_1^2 \\ D^2 &= D^3 + 2v_1 \epsilon \\ C^3 &= \frac{1}{v_2 \sqrt{1-\rho^2}} \left( \mu_2 - \log(R+K) + \frac{v_1 R}{R+K} y_0 - \frac{1}{2} \frac{v_1^2 R K}{(R+K)^2} y_0^2 \right) \\ D^3 &= \frac{1}{v_2 \sqrt{1-\rho^2}} \left( \rho v_2 - \frac{v_1 R}{R+K} + \frac{v_1^2 R K}{(R+K)^2} y_0 \right) \\ \epsilon &= -\frac{1}{2v_2 \sqrt{1-\rho^2}} \frac{v_1^2 R K}{(R+K)^2}\end{aligned}$$

where:

$$R = e^{v_1 y_0 + \mu_1}$$

### 4.2.3 Numerical Methods

**Numerical Integration** An analytical expression for the probability density of the spread between to log-normally distributed random variables does not exist. However, due to the fact that when we condition a normal random variable on another correlated normal random variable the distribution remains normal, we can employ a conditioning technique to simplify the pricing equation (1). The conditioning technique transforms the two-dimensional integral, representing the expectation taken under the martingale measure, into a one-dimensional integral. We will use the same representation as Deng, Li and Zhou [13], in which the price of the spread option is given by equation (11). The integrals are then solved numerically using a global adaptive quadrature method. The price produced by this procedure will be used as a benchmark when the accuracy of the other pricing methods is evaluated.

**Monte Carlo Simulation** Monte Carlo integration is a fundamental approach to estimating an expectation given by  $\tau = \mathbb{E}(\varphi(X)) = \int \varphi(x)f(x)dx$ , where  $f$  is the probability density of  $X$ . The method is a numerical method for integration based on the law of large numbers. The estimation is carried out according to algorithm 2, for more background on Monte Carlo integration see Sköld [18].

---

**Algorithm 2** Monte Carlo integration

---

1. Draw  $N$  values  $x_1, \dots, x_N$  independently from  $f$
2. Approximate  $\tau = \mathbb{E}(\varphi(X))$  by:

$$t_N = t(x_1, \dots, x_N) = \frac{1}{N} \sum_{i=1}^N \varphi(x_i)$$


---

The expectation in the pricing equation (1) can always be approximated using Monte Carlo methods. The basic principle of the method is simple, we simulate a large number of paths of the asset processes  $S_1$  and  $S_2$  in the interval  $[0, T]$  and for each pair of simulated paths we calculate the payoff at time to maturity  $T$ , given by  $S(T) = (S_2(T) - S_1(T) - K)^+$ . The expectation in the pricing equation is then approximated by the sample average of the generated payoffs for the contract. Since we know that under the 2-factor GBM framework the terminal joint distribution is bivariate normal we can simulate the underlying asset values at maturity directly and therefore it is not necessary to simulate complete index paths, one single time step is adequate. The values of the indexes  $S_1$  and  $S_2$  at time to maturity  $T$  are then given by:

$$S_1(T) = S_1(0) \exp \left[ \left( r - \delta_1 - \frac{1}{2} \sigma_1^2 \right) T + \sigma_1 \sqrt{T} (\rho Z_2 + \sqrt{1 - \rho^2} Z_1) \right]$$

$$S_2(T) = S_2(0) \exp \left[ \left( r - \delta_2 - \frac{1}{2} \sigma_2^2 \right) T + \sigma_2 \sqrt{T} Z_2 \right]$$

where  $Z_1$  and  $Z_2$  are two independent standard normal random variables.

Although it is fairly easy to simulate these processes and get an estimate of the price, the challenges with the method lies in controlling the error of the approximation. Various so called variance reduction procedures have been developed to improve the accuracy of the estimation. Control variates, antithetic variates and importance sampling are examples of this. Below we will outline the approach of antithetic variates.

**Antithetic Variates** Suppose that we want to estimate  $\tau = \mathbb{E}[\varphi(X)] = E[Z]$  and that we have two generated samples  $Z_1$  and  $Z_2$  with the same distribution and means  $\hat{\tau}_1 = \hat{\tau}_2$ . An unbiased estimator of  $\tau$  is then:

$$\hat{\tau} = \frac{\hat{\tau}_1 + \hat{\tau}_2}{2}$$

and the variance is given by:

$$\begin{aligned} Var[Z] &= Var\left[\frac{Z_1 + Z_2}{2}\right] = \frac{1}{4}(Var[Z_1] + Var[Z_2] + 2Cov[Z_1, Z_2]) \\ &= \frac{Var[Z_1]}{2} + \frac{Cov[Z_1, Z_2]}{2} \end{aligned}$$

In the above equation we note that the variance of the estimator is reduced if  $Cov[Z_1, Z_2] < 0$ . This implies that if we can find a sample path that has the same mean but is negatively correlated with the sample path we want to estimate we can produce an estimator with a reduced variance and thereby an improved accuracy.

In our case this is fairly straightforward to do. When we simulate the asset prices we generate two vectors of independent standard normal random variables  $Z_1$  and  $Z_2$ . By forming the antithetic vectors  $-Z_1$  and  $-Z_2$  we can compute two different sets of final asset price vectors, the real asset prices and the antithetic asset prices. Next we compute the payoff vector in both cases,  $\phi_1$  and  $\phi_2$ , and calculate the average between the normal and the antithetic payoffs. We then estimate the price  $p$  of the spread option as the discounted average payoff:

$$p = e^{-rT} \frac{1}{N} \sum_{i=1}^N \left( \frac{\phi_1(i) + \phi_2(i)}{2} \right)$$

Due to the fact that the two sets of random variables are negatively correlated this will lead to a more accurate estimate of the price than the original one.

**Fourier Methods** Pricing methods based on the Fourier transform use the characteristic function of the log-price process to retrieve an expression of the price that can be approximated using the fast Fourier transform, or some other transform method. The FFT method implemented in this thesis was reviewed in section 3. A great advantage of the FFT method is that calculating the spread option price under different market models only amounts to changing the characteristic function  $\Phi$  in equation (8).

In the 2-GBM model the joint characteristic function of  $X_T = (\log S_1(T), \log S_2(T))$  is of the form  $e^{iuX'_0} \Phi_T(u)$  with

$$\Phi_T(u) = \exp\left[(iu(rTe - \sigma^2 T/2))' - u\Sigma u'T/2\right]$$

where  $u = (u_1, u_2)$ ,  $e = (1, 1)$ ,  $\Sigma = [\sigma_1^2, \sigma_1\sigma_2\rho; \sigma_1\sigma_2\rho, \sigma_2^2]$  and  $\sigma^2 = \text{diag}\Sigma$ .

### 4.3 Stochastic Volatility

The stochastic volatility model is set up as the following, with  $X_i = \log S_i$  we have the dynamics:

$$dX_1 = (r - \delta_1 - \frac{1}{2}\sigma_1^2 v)dt + \sigma_1 \sqrt{v} d\mathbf{W}_1$$

$$dX_2 = (r - \delta_2 - \frac{1}{2}\sigma_2^2 v)dt + \sigma_2 \sqrt{v} d\mathbf{W}_2$$

$$dv = \kappa(\mu - v)dt + \sigma_v \sqrt{v} d\mathbf{W}_v$$

where

$$\mathbb{E}^{\mathbb{Q}}[d\mathbf{W}_1 d\mathbf{W}_2] = \rho dt$$

$$\mathbb{E}^{\mathbb{Q}}[d\mathbf{W}_1 d\mathbf{W}_v] = \rho_1 dt$$

$$\mathbb{E}^{\mathbb{Q}}[d\mathbf{W}_2 d\mathbf{W}_v] = \rho_2 dt$$

As stated earlier this is a multivariate extension of the single-asset Heston stochastic volatility model suggested by Heston [9] where the volatility process is modeled as a Cox-Ingersoll-Ross (CIR) process first introduced by Cox, Ingersoll and Ross [6] as a short rate model. In the multivariate setting we let the volatilities for the underlying indexes be proportional to this volatility process. In the dynamics for  $v$  we note that the process is mean-reverting towards the so called long variance  $\mu$ . Furthermore,  $\kappa$  governs the rate at which  $v$  reverts to  $\mu$ , and  $\sigma_v$  determines the volatility of the process. Lastly the volatility process is strictly positive if the parameters satisfies the *Feller condition*  $2\kappa\mu > \sigma_v^2$ .

As we introduce a stochastic structure for the volatilities, the conditioning technique is no longer available since we have moved out of the Gaussian territory. Additionally, there are no analytical closed form approximations available for the price of the spread option under this model, which means that we are referred to numerical approaches.

#### 4.3.1 Fourier Methods

By applying Ito's lemma and solving the resulting PDE Dempster and Hong [7] derive the following analytical expression for the joint characteristic function  $e^{iuX'_0}\Phi_T(u)$ :

$$\begin{aligned} \Phi_T^{(SV)}(u) = & \exp \left[ \left( \frac{2\zeta(1 - e^{-\theta T})}{2\theta - (\theta - \gamma)(1 - e^{-\theta T})} \right) v(0) \right. \\ & \left. + iu(re - \delta)'T - \frac{\kappa\mu}{\sigma_v^2} \left[ 2\log \left( \frac{2\theta - (\theta - \gamma)(1 - e^{-\theta T})}{2\theta} \right) + (\theta - \gamma)T \right] \right] \end{aligned}$$

where

$$\zeta = -\frac{1}{2} [(\sigma_1^2 u_1^2 + \sigma_2 u_2^2 + 2\rho\sigma_1\sigma_2 u_1 u_2) + i(\sigma_1^2 u_1 + \sigma_2^2 u_2)]$$

$$\gamma = \kappa - i(\rho_1\sigma_1 u_1 + \rho_2\sigma_2 u_2)\sigma_v$$

$$\theta = \sqrt{\gamma^2 - 2\sigma_v^2 \zeta}$$

$$e = (1, 1)$$

### 4.3.2 Monte Carlo Simulation

Under the stochastic volatility model the terminal joint distribution of the spread is not known, which means that we need to simulate complete paths of the underlying factors to get at it. This is done by applying an Euler discretization to the model defined in subsection 4.3, where again  $X_i = \log S_i$ :

$$X_i(t + \Delta t) = X_i(t) + (r - \delta_i - \frac{1}{2}\sigma_i^2 v(t))\Delta t + \sigma_i \sqrt{v(t)} \Delta \mathbf{W}_i, i = 1, 2$$

$$v(t + \Delta t) = v(t) + \kappa(\mu - v(t))\Delta t + \sigma_v \sqrt{v(t)} \Delta \mathbf{W}_v$$

By discretizing the process as above we introduce a discretization error which means that it is now possible for the process to attain negative values. This is of course not desirable and is avoided by applying a so called *full truncation* scheme. The volatility process now becomes:

$$v(t + \Delta t) = v(t) + \kappa(\mu - v(t)^+)\Delta t + \sigma_v \sqrt{v(t)^+} \Delta \mathbf{W}_v$$

where  $v(t)^+ = \max(0, v(t))$ .

In order to simulate the Brownian motions we use the fact that an increment of a Wiener process is normally distributed with standard deviation  $\sqrt{\Delta t}$  along with the knowledge that the increments are independent, this means that we can substitute  $\Delta \mathbf{W}$  with  $\sqrt{\Delta t}Z$  where  $Z$  is a standard normal distributed random variable. To simulate the correlated Brownian motions we only need to simulate correlated normal random variables, which is done using the Cholesky decomposition of the covariance matrix. Let  $\Sigma$  be the covariance matrix and  $C$  its Cholesky decomposition, then we can generate normal random variables correlated according to  $\Sigma$  as:

$$Y = CZ, Z \in N(0, 1)$$

Our model can now be simulated as:



$$\begin{aligned}
v(t + \Delta t) &= v(t) + \kappa(\mu - v(t)^+) \Delta t + \sqrt{v(t)^+} \sqrt{\Delta t} Y(1, 1) \\
X_1(t + \Delta t) &= X_1(t) + (r - \delta_1 - \frac{1}{2} \sigma_1^2 v(t)) \Delta t + \sqrt{v(t)} \sqrt{\Delta t} Y(2, 1) \\
X_2(t + \Delta t) &= X_2(t) + (r - \delta_2 - \frac{1}{2} \sigma_2^2 v(t)) \Delta t + \sqrt{v(t)} \sqrt{\Delta t} Y(3, 1)
\end{aligned}$$

where  $Y(i, j)$  denotes the  $i$ 'th row and  $j$ 'th column of the matrix  $Y = CZ$ ,  $Z \in N(0, 1)$ , and  $C$  is the (lower triangular) Cholesky decomposition of the covariance matrix  $\Sigma$  defined by:

$$\Sigma = \begin{bmatrix} \sigma_v^2 & \sigma_v \sigma_1 \rho_1 & \sigma_v \sigma_2 \rho_2 \\ \sigma_1 \sigma_v \rho_1 & \sigma_1^2 & \sigma_1 \sigma_2 \rho \\ \sigma_2 \sigma_v \rho_2 & \sigma_2 \sigma_1 \rho & \sigma_2^2 \end{bmatrix}$$

#### 4.4 Stochastic Volatility and Jump Diffusion

We now extend the stochastic volatility model further by including random jumps in the asset processes. The jumps are assumed to be independent from the diffusion process. The risk neutral dynamics are then given by:

$$\begin{aligned}
dS_1 &= S_1(r - \delta_1)dt + \sigma_1 \sqrt{v} S_1 d\mathbf{W}_1 + S_1 dJ_1 \\
dS_2 &= S_2(r - \delta_2)dt + \sigma_2 \sqrt{v} S_2 d\mathbf{W}_2 + S_2 dJ_2 \\
dv &= \kappa(\mu - v)dt + \sigma_v \sqrt{v} d\mathbf{W}_v
\end{aligned}$$

$$\mathbb{E}^{\mathbb{Q}}[d\mathbf{W}_1 d\mathbf{W}_2] = \rho dt$$

$$\mathbb{E}^{\mathbb{Q}}[d\mathbf{W}_1 d\mathbf{W}_v] = \rho_1 dt$$

$$\mathbb{E}^{\mathbb{Q}}[d\mathbf{W}_2 d\mathbf{W}_v] = \rho_2 dt$$

Again this can be seen as a multivariate generalization of the single-asset Bates model proposed by Bates [1]. The process  $J(t) = (J_1(t), J_2(t))$  is defined as a compound Poisson process that delivers simultaneous jumps where the jump sizes  $k$  are multivariate log-normally distributed as  $\log(1+k) \in N(z, \varphi)$  arriving according to a Poisson process with some intensity factor  $\lambda$ . The parameters that are being added to the model are:

$$z = [z_1, z_2]$$

$$\varphi = \begin{bmatrix} q_1^2 & q_1 q_2 \rho_{Jumps} \\ q_1 q_2 \rho_{Jumps} & q_2^2 \end{bmatrix}$$

where  $z_1, z_2$  set the mean jump sizes and  $q_1, q_2$  specify the jump size volatility for the two underlying asset processes. Furthermore, we need to specify the

jump intensity factor  $\lambda$  and a correlation coefficient governing the correlation between the jump sizes  $\rho_{Jumps}$ .

By applying Ito's formula to the log-price  $X_i = \log S_i$  the following dynamics for  $X_i$  can be derived, see Lindström, Madsen and Nielsen [12]:

$$dX_i = (r - \delta_i - \lambda \left( e^{z_i + \frac{q_i^2}{2}} - 1 \right) - \frac{1}{2} \sigma_i^2 v) dt + \sigma_i \sqrt{v} d\mathbf{W}_i + dJ_i$$

where the term  $\lambda \left( e^{z_i + \frac{q_i^2}{2}} - 1 \right)$  is a drift correction term arising from the jump process in order for discounted price process to still be a martingale under the risk neutral measure.

#### 4.4.1 Fourier Methods

Since the jumps added to our model are independent from the continuous part of the process, the joint characteristic function  $e^{iuX'_0} \Phi_T(u)$  is given by:

$$\Phi_T(u) = \Phi_T^{(SV)}(u) \Phi_T^{(Jumps)}(u)$$

where  $\Phi_T^{(SV)}(u)$  is given in subsection 4.3.1. Note that we need to include the drift correction term  $\lambda \left( e^{z_i + \frac{q_i^2}{2}} - 1 \right)$ .

The characteristic function for the jump process in the single asset case is given by Lindström, Madsen and Nielsen [12], from this it is straightforward to see that in the bivariate case  $\Phi_T^{(Jumps)}(u)$  is given by:

$$\Phi_T^{(Jumps)}(u) = e^{t\lambda(e^{iu_1 z_1 - \frac{u_1^2 q_1^2}{2}} - 1)}$$

#### 4.4.2 Monte Carlo Simulation

Simulation of the model is performed in a similar fashion to the simulation of the stochastic volatility model described in subsection 4.3.2. Since the jumps are independent of the continuous parts of the processes, we can simulate the compound Poisson jump process first. This is done by generating two jump vectors  $J_1(t)$  and  $J_2(t)$ . First the jump times are simulated as a Poisson process with intensity factor  $\lambda$ . If a jump occurs at time  $t$ ,  $J(t) = (J_1(t), J_2(t))$  is set to be the generated jump sizes drawn from the multivariate normal distribution defined by the jump process parameters. On the other hand if no jump occurs at time  $t$   $J_i(t)$  for  $i = 1, 2$  is equal to zero. The model can now be simulated as the following, again using an Euler discretization with a full truncation scheme applied to the volatility process:

$$\begin{aligned} v(t + \Delta t) &= v(t) + \kappa(\mu - v(t)^+) \Delta t + \sqrt{v(t)^+} \sqrt{\Delta t} Y(1, 1) \\ X_1(t + \Delta t) &= X_1(t) + (r - \delta_1 - \lambda \left( e^{z_1 + \frac{q_1^2}{2}} - 1 \right) - \frac{1}{2} \sigma_1^2 v(t)) \Delta t + \sqrt{v(t)} \sqrt{\Delta t} Y(2, 1) + J_1(t) \end{aligned}$$

$$X_2(t+\Delta t) = X_2(t) + (r - \delta_2 - \lambda) \left( e^{z_2 + \frac{q_2^2}{2}} - 1 \right) - \frac{1}{2} \sigma_2^2 v(t) \Delta t + \sqrt{v(t)} \sqrt{\Delta t} Y(3, 1) + J_2(t)$$

where  $X_i = \log S_i$ ,  $Y(i, j)$  denotes the  $i$ 'th row and  $j$ 'th column of the matrix  $Y = CZ$ ,  $Z \in N(0, 1)$ , and  $C$  is the (lower) Cholesky decomposition of the covariance matrix  $\Sigma$  defined by:

$$\Sigma = \begin{bmatrix} \sigma_v^2 & \sigma_v \sigma_1 \rho_1 & \sigma_v \sigma_2 \rho_2 \\ \sigma_1 \sigma_v \rho_1 & \sigma_1^2 & \sigma_1 \sigma_2 \rho \\ \sigma_2 \sigma_v \rho_2 & \sigma_2 \sigma_1 \rho & \sigma_2^2 \end{bmatrix}$$

## 5 Numerical Results

In this section we review the numerical results. The section is divided by market models. In subsection 5.1 we look at the performance of the FFT method in the 2-GBM framework. In the next section we move on to the case of stochastic volatility and lastly in section 5.3 we evaluate the pricing method when random jumps are added to the model. In all cases we test the accuracy and the computational speed of the method. Furthermore, we test the sensitivity to the parameters one need to specify in order to implement the FFT pricing method. In addition to this we look at the price sensitivity to the various market parameters. All the code is implemented in MATLAB version R2014b and is run on Mac OS X Lion 10.7.5 on a 2.3 GHz Intel Core i5 processor with 4 gigabytes of memory.

### 5.1 Geometric Brownian Motion

In table 1 we compare the prices from the FFT method to the benchmark prices produced by numerical integration. The prices are calculated under a benchmark set of parameters and the damping parameters are fixed at  $(\epsilon_1, \epsilon_2) = (-3, 1)$ . The truncation parameter is set to be  $\bar{u}_{min} = 40$  but the actual integration interval is calculated using algorithm 1. The errors are actual errors defined by  $price_{FFT} - price_{Benchmark}$ .

We see that the pricing method produces accurate prices across all choices of discretization points  $N$ . Although, it seems to be significantly less accurate for  $N = 128$  and  $N = 256$ . However, it will be shown in subsection 5.1.2 that these errors can be notably reduced by tuning the parameter  $\bar{u}_{min}$  thereby changing the step size which leads to a lower discretization error. The errors for the finest grids,  $N = 1024$  and  $N = 2048$  can also be somewhat reduced by choosing a larger integration interval, lowering the truncation error. It is also worth noting that the price produced by the FFT (for the finer grids) is lower than the benchmark price across all strikes.

In table 2 we look at the computational effort for different choices of discretization grids. The damping parameters and the integration interval remains the same as before  $(\epsilon_1, \epsilon_2) = (-3, 1)$  and  $\bar{u}_{min} = 40$  but 100 different spread

Table 1: FFT prices compared to the benchmark produced by numerical integration for various strike prices  $K$ . The parameters are  $\bar{u}_{min} = 40, (\epsilon_1, \epsilon_2) = (-3, 1), S_1(0) = 96, S_2(0) = 100, r = 0.05, \sigma_1 = 0.1, \sigma_2 = 0.2, T = 1, \rho = 0.5, \delta_1 = 0, \delta_2 = 0$ .

<b>K</b>	<b>Num. Int</b>	<b>N=128</b>	<b>N=256</b>	<b>N=512</b>	<b>N=1024</b>	<b>N=2048</b>
1	8.4286	5.5579e-3	2.8399e-7	-4.3698e-13	-4.2455e-13	-6.6080e-13
2	7.9290	5.4896e-3	2.7866e-7	-5.8975e-13	-6.4926e-13	-8.8107e-13
3	7.4510	5.7514e-3	3.0769e-7	-6.2350e-13	-7.6472e-13	-7.0166e-13
4	6.9942	5.3655e-3	2.6932e-7	-9.3525e-13	-9.5213e-13	-8.0647e-13
5	6.5584	6.6620e-3	4.1810e-7	-4.6629e-13	-4.5830e-13	-3.7215e-13
6	6.1433	5.6425e-3	3.0155e-7	-6.2528e-13	-5.7554e-13	-6.7679e-13
7	5.7484	5.6062e-3	2.9950e-7	-4.7429e-13	-4.7606e-13	-4.7873e-13
8	5.3734	6.9256e-3	4.6047e-7	-2.5047e-13	-3.1086e-13	-1.9718e-13
9	5.0178	6.0070e-3	3.4828e-7	-1.5721e-13	-1.3856e-13	-1.3234e-13
10	4.6811	6.7448e-3	4.4221e-7	-7.6383e-14	-1.4388e-13	-3.8192e-13

options are generated randomly and the time is an average computational time taken over these 100 options.

Table 2: Average computational time for the FFT method under the 2-GBM framework in seconds taken over 100 randomly generated spread options.

Discretization	Comp. time (s)
N=128	0.04
N=265	0.13
N=512	0.54
N=1024	2.12
N=2048	8.54

### 5.1.1 Accuracy & Speed

To evaluate the performance of the FFT pricing method we perform a systematic test which is inspired by, and for comparison reasons very similar to, the procedure carried out by Deng, Li and Zhou [13]. We start by generating a number of spread options, since the short rate  $r$  is deemed to be fairly insignificant it is held constant at 5% and since the continuous dividend yields  $\delta_1$  and  $\delta_2$  can be absorbed by  $r$  these are set to zero. To let the moneyness of the options vary we hold  $S_2$  constant at  $S_2 = 100$  while  $S_1$  is drawn uniformly so that  $S_1/S_2 \in [0.7, 1.2]$ . Similarly, we set the range of  $K/S_2$  to be  $[0.01, 40]$  and that of the volatility parameters to be  $\sigma_i \in [0.1, 0.8]$ . Additionally, the interval for the correlation is  $\rho \in [-0.75, 0.75]$  and since  $\sqrt{T}$  always is accompanied by

$\sigma_i$ 's, the time to maturity is set to be  $T = 1$ . Lastly, to rule out very far out of the money options we enforce the following constraint:  $S_2 - S_1 - Ke^{-rT} \geq 30$ .

Having randomly generated a set of options we test the accuracy by pricing the options with the FFT method, the closed form approximation proposed by Deng, Li and Zhou, the classic approximation by Kirk, a Monte Carlo simulation (100,000 simulations) with antithetic variates for variance reduction and, for reference, the Bachelier model. We then compare these approximations to the benchmark calculated by numerical integration. To make the comparison we define some error estimators; the mean absolute percentage error (MAPE), the mean percentage error (MPE) and the mean squared error (MSE) for pricing method  $j$ , where  $N$  is the number of options, are defined as follows:

$$MAPE_j = \frac{1}{N} \sum_{i=1}^N \left| \frac{p_i^j - p_i^{Benchmark}}{p_i^{Benchmark}} \right|$$

$$MPE_j = \frac{1}{N} \sum_{i=1}^N \frac{p_i^j - p_i^{Benchmark}}{p_i^{Benchmark}}$$

$$MSE_j = \frac{1}{N} \sum_{i=1}^N (p_i^j - p_i^{Benchmark})^2$$

We concentrate on the relative errors since the prices tend to vary quite intensively. The MAPE will be the preferred measure, the MPE will give additional information regarding the bias, and the MSE will give some insight into the actual errors. In addition we measure the median of the absolute percentage error and the median as well as the minimum and the maximum of the percentage error. For the results of the accuracy evaluation see table 3. The number of generated options is 1000. The computational time is again calculated as an average time per option taken over 100 randomly generated options.

Studying table 3 there are a couple things worth discussing. Firstly we note that the FFT method is the most accurate of the tested pricing approaches, even at the  $N = 128$  level, beating the competition on every measure we look at. We also note that the benefit from increasing the discretization seem to be small, although the median of the error stands out. In terms of accuracy the closed-form approximation proposed by Deng, Li and Zhou also performs well, at a much smaller computational expense than the FFT. This is not surprising considering the nature of the two approaches and it falls in line with the general spread option valuation challenge, analytical closed-form approximations tend to be quick while numerical approaches are more accurate. This presents a trade-off between accuracy and speed. The same reasoning holds true for Kirk's approximation as well, which is even quicker, although much less accurate. It is also worth pointing out that Kirk's approximation seems to be biased, constantly producing prices that are greater than the benchmark.

Additionally, we should consider the fact that the FFT method gives a grid ( $N^2$ ) of prices at the same time, which means that if we want to price several

Table 3: Accuracy and speed of the different pricing methods. The number of generated spread options is 1000. The FFT parameters are  $(\epsilon_1, \epsilon_2) = (-3, 1)$  and  $\bar{u}_{min} = 20$ . DLZ represents the Deng, Li, Zhou approximation.

	<b>Bachelier</b>	<b>Kirk's</b>	<b>DLZ</b>	<b>FFT(N=128)</b>	<b>FFT(N=256)</b>	<b>MC(N=100000)</b>
<b>MAPE</b>	0.1454	2.6646e-2	3.1523e-4	8.2842e-6	7.5950e-6	2.7714e-3
Std(APE)	0.1372	3.128e-2	1.8724e-3	1.3334e-4	1.3345e-4	2.4620e-3
Median(APE)	0.1152	1.7065e-2	2.5240e-5	7.2035e-8	1.8223e-12	2.2175e-3
<b>MPE</b>	0.1372	2.6645e-2	1.6688e-4	-6.0306e-6	-6.7964e-6	-1.9876e-4
Std(PE)	0.1453	3.1280e-2	1.8914e-3	1.3346e-4	1.3349e-4	3.7027e-3
Median(PE)	0.1130	1.7065e-2	4.8101e-6	6.1877e-8	2.7127e-15	-1.4939e-4
max(PE)	1.2887	0.3474	1.6675e-2	2.2006e-4	2.1561e-4	1.2001e-2
min(PE)	-0.3581	-2.2751e-4	-4.7752e-2	-3.5166e-3	-3.5201e-3	-1.8259e-2
<b>MSE</b>	14.0681	0.2409	8.7833e-5	7.8396e-8	7.6813e-8	7.1175e-3
Comp.time (s)	0.0004	0.0005	0.002	0.04	0.13	0.07

options at the same it is not necessary to run the pricing algorithm for each option, instead we could find the appropriate prices by interpolating on the grid. This adds even more nuance to the trade-off. We note that we can price approximately 20 options individually using the Deng, Li, Zhou approximation before we reach the computational effort required to run the FFT method a single time with  $N = 128$ .

Lastly, the Deng, Li, Zhou approximation, being on closed form, has the advantage of being easier to implement and there is no need for any discretization or damping parameters to be specified.

To summarize, under the 2-GBM framework, the trade-off between different pricing approaches is not trivial and will oftentimes depend on what application we are considering it for. However, when we move on to more advanced market models we will see the real strength of the FFT method.

### 5.1.2 Sensitivity to the Discretization Parameters

In this section we analyze the sensitivity to the number of discretization points  $N$  and the parameter  $\bar{u}_{min}$ . Table 4 shows the mean relative error for different choices of  $\bar{u}_{min}$  and  $N$ . The error is calculated as an average based on 30 randomly generated options. The options were generated according to the same procedure as in the previous subsection. The choice of  $\bar{u}_{min}$  is essentially a trade-off between discretization error and truncation error, a higher value means a bigger integration interval which in turn leads to a smaller truncation error. However, a larger integration interval means a bigger step size, for a given number of discretization points  $N$ , which gives a bigger discretization error. The conclusion is that a higher  $N$  means that we can “afford” a bigger integration interval and therefore a lower truncation error. This is illustrated well in figure

1. This analysis gives great insight into the challenge of choosing these parameters when implementing the method. It is worth noting that the benefit from increasing the discretization above  $N = 256$  is small according to this measure.

In conclusion, our method is not deemed to be very sensitive to the choice of discretization and truncation parameters, but given the analysis it is possible to make a more optimal choice setting up the model. One wants to make sure not to choose an integration interval that is “too large” for the number of discretization points, in which case the error caused by the discretization dominates. This is the reason why the error is significantly higher for the less fine grids in table 1.

Table 4: Mean absolute relative error (MAPE) for different choices of  $\bar{u}_{min}$  and discretization  $N$ . The MAPE is calculated based on 30 randomly generated options.

<b>u_min</b>	<b>N</b>			
	<b>128</b>	<b>256</b>	<b>512</b>	<b>1024</b>
<b>20</b>	3.0978e-8	2.9163e-9	2.9163e-9	2.9163e-9
<b>40</b>	3.2940e-4	1.9832e-8	2.9163e-9	2.9163e-9
<b>60</b>	-	1.2310e-5	2.8839e-9	2.9163e-9
<b>80</b>	-	3.2940e-4	1.9832e-8	2.9163e-9
<b>100</b>	-	-	9.7839e-7	2.9161e-9
<b>120</b>	-	-	1.2310e-5	2.8839e-9
<b>140</b>	-	-	8.0993e-5	1.5231e-9
<b>160</b>	-	-	3.1294e-4	1.7619e-8
<b>200</b>	-	-	-	9.1566e-7
<b>240</b>	-	-	-	1.8884e-5
<b>280</b>	-	-	-	1.1971e-4

### 5.1.3 Sensitivity to the Damping Parameters

In order to implement the FFT method we also need to specify the damping parameters  $(\epsilon_1, \epsilon_2)$  which are introduced to make sure the option price is square-integrable. The requirements on these parameters stated by Hurd and Zhou [10] is that  $\epsilon_2 > 0$  and  $\epsilon_1 + \epsilon_2 < -1$ , which essentially make sure we avoid singularities. Although, the results in this thesis suggest that we want to be more careful than that in choosing  $\epsilon = (\epsilon_1, \epsilon_2)$ . The mean absolute relative error for different choices of  $\epsilon$  is given in table 5. This is also illustrated graphically in figure 2. The analysis points out that we start seeing an increase in the error when we approach the boundaries given by the conditions mentioned above. Based on the numbers this author suggest that we instead choose  $\epsilon$  so that  $\epsilon_2 \geq 0.6$  and  $\epsilon_1 + \epsilon_2 \leq -1.6$ . Furthermore, we do not want to pick a too large negative value for  $\epsilon_1$  as this also increases the error function (although relatively insignificant),  $\epsilon_1 > -4$  seems reasonable.

However, keeping this rule of thumb in mind, we can conclude that the

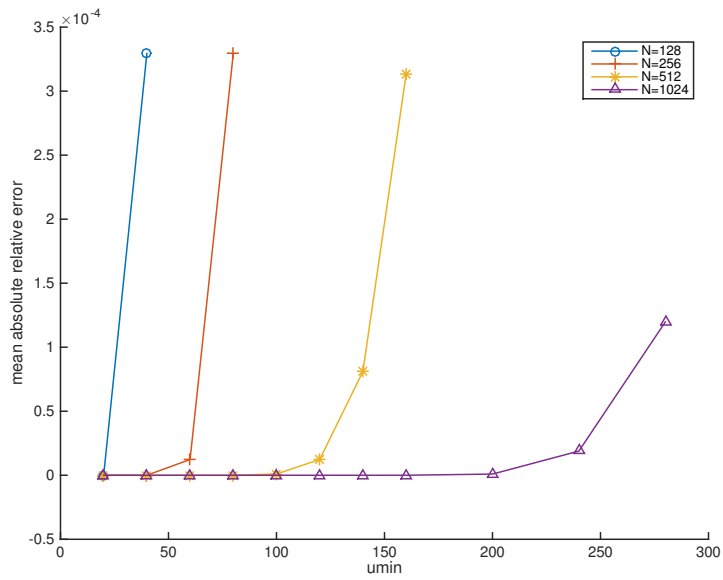


Figure 1: Mean absolute relative error (MAPE) for different choices of  $\bar{u}_{min}$  and discretization  $N$ . The MAPE is calculated based on 30 randomly generated options.

method is not very sensitive to the choice of damping parameters. But again, we are able to make a more or less optimal choice, and thereby influence the performance of the pricing method.



Table 5: Mean absolute relative error (MAPE) for different choices of damping parameters  $\epsilon = (\epsilon_1, \epsilon_2)$  under the 2-GBM market model. The MAPE is calculated based on 30 randomly generated options.

$\epsilon_2/\epsilon_1$	-4.4	-4.2	-4.0	-3.8	-3.6	-3.4	-3.2	-3.0	-2.8	-2.6	-2.4	-2.2	-2.0	-1.8	-1.6	-1.4
0.2	5.40e-3	5.41e-3	5.41e-3	5.41e-3	5.42e-3	5.42e-3	5.42e-3	5.42e-3	5.42e-3	5.42e-3	5.42e-3	5.42e-3	5.42e-3	5.42e-3	5.42e-3	6.05e-3
0.4	2.91e-6	2.94e-6	2.96e-6	2.97e-6	2.98e-6	2.98e-6	2.98e-6	2.98e-6	2.98e-6	2.98e-6	2.98e-6	2.98e-6	2.98e-6	2.98e-6	3.19e-6	4.41e-4
0.6	5.32e-8	4.44e-8	3.72e-8	3.10e-8	2.61e-8	2.18e-8	2.21e-8	2.24e-8	2.17e-8	2.04e-8	1.89e-8	1.74e-8	1.76e-7	3.35e-4	-	-
0.8	5.10e-8	4.22e-8	3.49e-8	2.86e-8	2.36e-8	1.94e-8	1.96e-8	1.98e-8	1.91e-8	1.78e-8	1.63e-8	1.48e-7	2.78e-4	-	-	-
1.0	5.04e-8	4.15e-8	3.42e-8	2.79e-8	2.29e-8	1.87e-8	1.88e-8	1.90e-8	1.83e-8	1.70e-8	1.35e-7	2.47e-4	-	-	-	-
1.2	4.96e-8	4.07e-8	3.34e-8	2.71e-8	2.23e-8	1.83e-8	1.86e-8	1.88e-8	1.80e-8	1.31e-7	2.33e-4	-	-	-	-	-
1.4	4.87e-8	4.01e-8	3.34e-8	2.77e-8	2.31e-8	1.91e-8	1.94e-8	1.97e-8	1.35e-7	2.30e-4	-	-	-	-	-	-
1.6	4.91e-8	4.09e-8	3.42e-8	2.85e-8	2.39e-8	1.99e-8	2.02e-8	1.44e-7	2.38e-4	-	-	-	-	-	-	-
1.8	4.98e-8	4.16e-8	3.49e-8	2.91e-8	2.45e-8	2.06e-8	1.58e-7	2.54e-4	-	-	-	-	-	-	-	-
2.0	5.04e-8	4.22e-8	3.54e-8	2.96e-8	2.50e-8	1.76e-7	2.81e-4	-	-	-	-	-	-	-	-	-
2.2	5.07e-8	4.25e-8	3.57e-8	3.00e-8	1.99e-7	3.19e-4	-	-	-	-	-	-	-	-	-	-
2.4	5.09e-8	4.26e-8	3.59e-8	2.98e-7	3.71e-4	-	-	-	-	-	-	-	-	-	-	-
2.6	5.08e-8	4.27e-8	2.95e-7	4.41e-4	-	-	-	-	-	-	-	-	-	-	-	-
2.8	5.07e-8	3.08e-7	5.34e-4	-	-	-	-	-	-	-	-	-	-	-	-	-
3.0	4.65e-7	6.57e-4	-	-	-	-	-	-	-	-	-	-	-	-	-	-

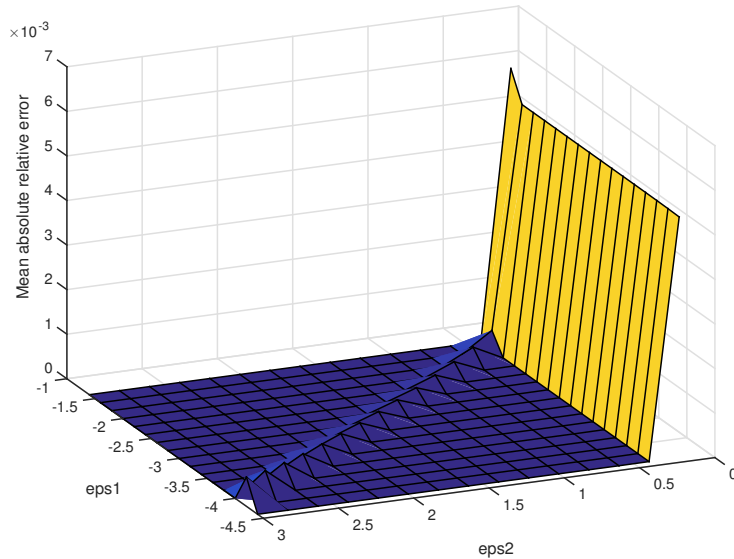


Figure 2: Mean absolute relative error (MAPE) for different choices of damping parameters  $\epsilon = (\epsilon_1, \epsilon_2)$  illustrated graphically. The MAPE is calculated based on 30 randomly generated options.

## 5.2 Stochastic Volatility

### 5.2.1 Accuracy & Speed

Since the conditioning technique is not available under the stochastic volatility model, and no other method is deemed accurate enough to serve as a benchmark we will evaluate the accuracy of the FFT method against a Monte Carlo simulation. For the simulation to be considered accurate enough we use 1,000,000 simulations with a discretization of 2,000 time steps. However, it is important to understand that we evaluate the performance against a benchmark that is in itself inaccurate, though we are able to quantify this uncertainty.

In table 6 we compare the prices produced by the FFT method with the benchmark for different strike prices  $K$ . We also include the standard errors for the benchmark. The prices are calculated using a benchmark set of parameters with a truncation interval  $\bar{u}_{min} = 40$  and the damping coefficients fixed at  $\epsilon = (-3, 1)$ . The benchmark set of parameters are:  $S_1 = 96$ ,  $S_2 = 100$ ,  $r = 0.1$ ,  $\delta_1 = 0.05$ ,  $\delta_2 = 0.05$ ,  $\sigma_1 = 0.5$ ,  $\sigma_2 = 1$ ,  $\rho = 0.5$ ,  $\rho_1 = 0.25$ ,  $\rho_2 = -0.5$ ,  $\sigma_v = 0.05$ ,  $v(0) = 0.04$ ,  $\kappa = 1.0$ ,  $\mu = 0.04$ ,  $T = 1$ . We see that the method gives accurate prices across the table. We also note that the actual error, defined

as  $price_{FFT} - price_{Benchmark}$ , is somewhat larger for  $N = 128$ , however after  $N = 256$  the increase in accuracy from a finer discretization is very limited. Again, the performance can be increased by tuning  $\bar{u}_{min}$  to a given  $N$ , this is considered in subsection 5.2.2.

In table 7, the real strength of the FFT method is revealed. Since moving to a more complex market model only amounts to changing the joint characteristic function in the pricing algorithm the computational cost is not significantly impacted. The FFT method produces accurate prices in only a fraction of the time it takes to generate a price by simulation. Table 8 shows the computational speed for the Monte Carlo method under different numbers of simulations and discretization. It also presents the estimated price and its associated standard error for strike price  $K = 2$  under the benchmark set of parameters. For comparison we have included the benchmark price and the price calculated by the FFT method with a discretization of  $N = 128$ . It is worth mentioning that the focus of this thesis has not been to write efficient Monte Carlo code, and no variance reduction method is applied, which means that the simulations could be improved. However, the point is clear, we see that in order to produce accurate price estimates through simulation a tremendous computational effort is required, which will prove insufficient in any practical application.

Strike	MC		FFT					
	N=1e6, n=2000		N=128	N=256	N=512	N=1024	N=2048	
1	8.0335 (0.011)		7.30369794867869e-3	2.0137776674094e-3	2.01350734387873e-3	2.01350734438854e-3	2.01350734431927e-3	
1.5	7.7874 (0.011)		7.58507562354982e-3	2.06711346451005e-3	2.0668185416497e-3	2.0668185419801e-3	2.06681854205026e-3	
2	7.5464 (0.011)		7.36288317941014e-3	2.13700819459017e-3	2.1367429760204e-3	2.13674297645028e-3	2.13674297634014e-3	
2.5	7.3104 (0.011)		7.30334389594933e-3	2.21875303327934e-3	2.21850127172996e-3	2.21850127237921e-3	2.21850127231971e-3	
3	7.0795 (0.011)		7.72509601624005e-3	2.24996818228007e-3	2.2496753498995e-3	2.24967535018994e-3	2.24967535034004e-3	
3.5	6.8538 (0.011)		7.69640167690966e-3	2.23553458238968e-3	2.23524241787043e-3	2.23524241835982e-3	2.23524241846995e-3	
4	6.6331 (0.010)		7.24385130214955e-3	2.1361370385895e-3	2.13588074554938e-3	2.13588074608939e-3	2.1358807463594e-3	
4.5	6.4174 (0.010)		7.84849274216981e-3	2.05905363587977e-3	2.05872320828959e-3	2.0587232086795e-3	2.05872320876033e-3	
5	6.2067 (0.010)		8.39369963919978e-3	2.05184493432053e-3	2.05144707615013e-3	2.05144707641036e-3	2.05144707654981e-3	
5.5	6.0009 (0.010)		7.22954381905971e-3	2.02257573758935e-3	2.02230695540973e-3	2.02230695587957e-3	2.02230695597017e-3	
6	5.8001 (0.010)		7.36003130296048e-3	1.98866808703002e-3	1.98838115032007e-3	1.98838115069044e-3	1.98838115067002e-3	

Table 6: The table shows the actual errors of the FFT method compared to the benchmark prices under the stochastic volatility model. The benchmark is calculated using a Monte Carlo method with 1,000,000 simulations and 2,000 time steps. The standard errors of the benchmark are given in parenthesis. The benchmark set of parameters is:  $S_1 = 96$ ,  $S_2 = 100$ ,  $r = 0.1$ ,  $\delta_1 = 0.05$ ,  $\delta_2 = 0.05$ ,  $\sigma_1 = 0.5$ ,  $\sigma_2 = 1$ ,  $\rho = 0.5$ ,  $\rho_1 = 0.25$ ,  $\rho_2 = -0.5$ ,  $\sigma_v = 0.05$ ,  $v(0) = 0.04$ ,  $\kappa = 1.0$ ,  $\mu = 0.04$ ,  $T = 1$  and  $\bar{u}_{min} = 40$ ,  $\epsilon = (-3, 1)$ .

Table 7: This table shows the average computational time in seconds for the FFT method under the stochastic volatility model. The average is calculated over 100 randomly generated spread options.

Discretization	Comp. time (s)
N=128	0.058
N=265	0.188
N=512	0.789
N=1024	3.134
N=2048	12.08

Table 8: Computational speed along with an estimated price and its standard error for different Monte Carlo runs. The table shows that the FFT method produces a more accurate price with a much lower computational effort. The price is calculated for  $K = 2$  under the benchmark set of parameters.

Time Steps	1000			2000			FFT N=128	Benchmark
Simulations	10000	50000	100000	10000	50000	100000	-	-
Comp. time (s)	113.41	559.21	1140.33	226.23	1112.48	2267.28	0.058	-
Price	7.4724	7.4990	7.5610	7.5293	7.5394	7.5016	7.5479	7.5464
SE	0.1093	0.0491	0.0347	0.1077	0.0491	0.0344	-	0.0109

### 5.2.2 Sensitivity to the Discretization Parameters

We now look at how the accuracy of the FFT method depends on the choices of  $\bar{u}_{min}$  and  $N$  in the stochastic volatility case. Table 9 and figure 3 show the mean absolute relative error for different choices of truncation and discretization parameters. Due to the computational effort required to produce accurate benchmarks under this model, the analysis is not as refined as in the 2-GBM case. The error function is calculated on 19 options, covering a wide range of different initial moneyness. The parameters are:  $S_1 = 100$ ,  $S_2 = 110$ ,  $r = 0.1$ ,  $\delta_1 = 0.05$ ,  $\delta_2 = 0.05$ ,  $\sigma_1 = 0.5$ ,  $\sigma_2 = 1$ ,  $\rho = 0.5$ ,  $\rho_1 = 0.25$ ,  $\rho_2 = -0.5$ ,  $\sigma_v = 0.05$ ,  $v(0) = 0.04$ ,  $\kappa = 1.0$ ,  $\mu = 0.04$ ,  $T = 1$  and  $K = 2, 3, 4, \dots, 20$ . Studying table 9 it is clear that the method show a similar behavior as under the previous market model, although the errors are larger. As we increase the number of discretization points we can reduce the error function somewhat by increasing the integration interval and thereby reducing the truncation error. However, the gain from doing so is small and might not be worth the extra computational cost. We note that under this model the method is once again not very sensitive to the choice of discretization parameters, but one should be aware of the choice of truncation parameter  $\bar{u}_{min}$ , especially when running the method on the coarser grids, since a poor choice will lead to big discretization errors.

Table 9: Mean absolute relative error (MAPE) for different choices of  $\bar{u}_{min}$  and discretization  $N$  for the SV model. The MAPE is calculated based on 19 options of different moneyness.

<b>u_min</b>	<b>N</b>			
	<b>128</b>	<b>256</b>	<b>512</b>	<b>1024</b>
<b>20</b>	3.4444e-4	3.4407e-4	3.4402e-4	3.4401e-4
<b>40</b>	2.5955e-3	3.2762e-4	3.2744e-4	3.2744e-4
<b>60</b>	-	4.2454e-4	3.2744e-4	3.2744e-4
<b>80</b>	-	2.5955e-3	3.2762e-4	3.2744e-4
<b>100</b>	-	-	3.3524e-4	3.2744e-4
<b>120</b>	-	-	4.2454e-4	3.2744e-4
<b>140</b>	-	-	8.3755e-4	3.2745e-4
<b>160</b>	-	-	2.3622e-3	3.2758e-4
<b>200</b>	-	-	-	3.3423e-4
<b>240</b>	-	-	-	3.4562e-3
<b>280</b>	-	-	-	3.6776e-3

### 5.2.3 Sensitivity to the Damping Parameters

Lets consider the sensitivity to the damping parameters  $\epsilon = (\epsilon_1, \epsilon_2)$  under the stochastic volatility model. In table 10 the mean absolute relative error is calculated based on the same parameters and 19 options as in the previous subsection 5.2.2 given different choices of damping parameters. We see again that we want to impose some restrictions on the parameters in addition to the ones stated in theorem 1, to make sure we are not making a poor decision and hurting the accuracy of the computed prices. Studying table 10 we see that the error function converges to a value of approximately  $3.37e - 3$  in the region  $\epsilon_2 \geq 0.8$  and  $\epsilon_1 + \epsilon_2 \leq -1.6$ . The error function is illustrated graphically in figure 4.

Figure 3: Mean absolute relative error (MAPE) for different choices of  $\bar{u}_{min}$  and discretization  $N$  under the stochastic volatility model. The MAPE is calculated based on 19 options of different moneyness.

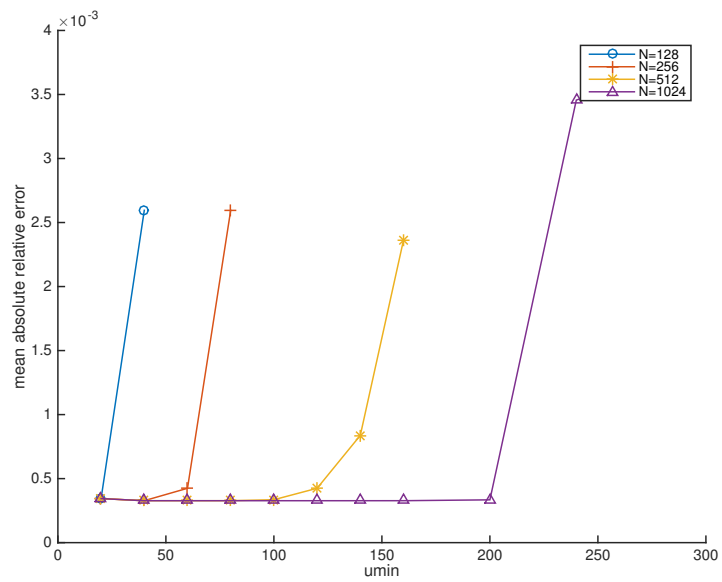


Table 10: This table shows the mean absolute relative error (MAPE) for different choices of damping parameters  $\epsilon = (\epsilon_1, \epsilon_2)$  under the stochastic volatility market model. The MAPE is calculated based on 19 options of different moneyness.

$\epsilon_2/\epsilon_1$	-4.4	-4.2	-4.0	-3.8	-3.6	-3.4	-3.2	-3.0	-2.8	-2.6	-2.4	-2.2	-2.0	-1.8	-1.6	-1.4
0.2	0.35	0.35	0.35	0.35	0.35	0.35	0.35	0.35	0.35	0.35	0.35	0.35	0.35	0.35	0.36	0.53
0.4	1.09e-2	1.09e-2	1.09e-2	1.09e-2	1.09e-2	1.09e-2	1.09e-2	1.09e-2	1.09e-2	1.09e-2	1.09e-2	1.09e-2	1.09e-2	1.34e-2	0.15	-
0.6	3.56e-3	3.56e-3	3.56e-3	3.56e-3	3.56e-3	3.56e-3	3.56e-3	3.56e-3	3.57e-3	3.57e-3	3.57e-3	3.62e-3	5.73e-3	0.12	-	-
0.8	3.38e-3	3.38e-3	3.38e-3	3.38e-3	3.38e-3	3.38e-3	3.38e-3	3.38e-3	3.23e-3	3.39e-3	3.43e-3	5.21e-3	9.86e-2	-	-	-
1.0	3.38e-3	3.37e-3	3.22e-3	3.37e-3	3.37e-3	3.37e-3	3.38e-3	3.38e-3	3.34e-3	3.42e-3	4.91e-3	8.26e-2	-	-	-	-
1.2	3.38e-3	3.37e-3	3.37e-3	3.37e-3	3.37e-3	3.37e-3	3.38e-3	3.38e-3	3.41e-3	4.67e-3	6.91e-2	-	-	-	-	-
1.4	3.38e-3	3.37e-3	3.37e-3	3.37e-3	3.37e-3	3.37e-3	3.38e-3	3.40e-3	4.46e-3	5.79e-2	-	-	-	-	-	-
1.6	3.38e-3	3.37e-3	3.37e-3	3.37e-3	3.37e-3	3.37e-3	3.39e-3	4.29e-3	4.88e-2	-	-	-	-	-	-	-
1.8	3.38e-3	3.37e-3	3.37e-3	3.37e-3	3.37e-3	3.39e-3	4.15e-3	4.18e-2	-	-	-	-	-	-	-	-
2.0	3.38e-3	3.37e-3	3.37e-3	3.37e-3	3.39e-3	4.03e-3	3.60e-2	-	-	-	-	-	-	-	-	-
2.2	3.38e-3	3.37e-3	3.37e-3	3.38e-3	3.63e-3	3.10e-2	-	-	-	-	-	-	-	-	-	-
2.4	3.38e-3	3.37e-3	3.38e-3	3.85e-3	2.69e-2	-	-	-	-	-	-	-	-	-	-	-
2.6	3.38e-3	3.38e-3	3.78e-3	2.24e-2	-	-	-	-	-	-	-	-	-	-	-	-
2.8	3.38e-3	3.72e-3	2.04e-2	-	-	-	-	-	-	-	-	-	-	-	-	-
3.0	3.67e-3	1.80e-2	-	-	-	-	-	-	-	-	-	-	-	-	-	-



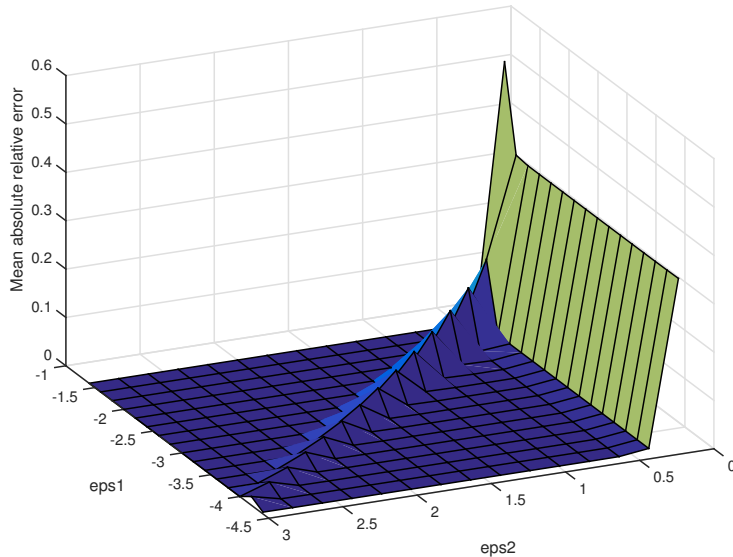


Figure 4: Mean absolute relative error (MAPE) for different choices of damping parameters  $\epsilon = (\epsilon_1, \epsilon_2)$  under the stochastic volatility model illustrated graphically. The MAPE is calculated based on 19 options.

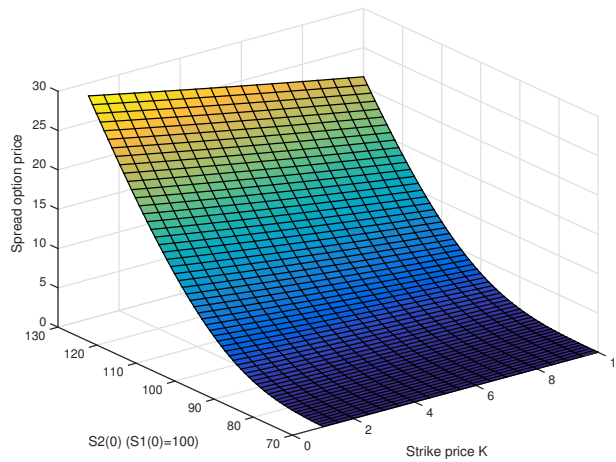
#### 5.2.4 Price Sensitivity to Market Parameters

The spread option price is a function of many parameters. We will now have a look at how the various market parameters influence the price. This is considered to be valuable information in order to understand how the model behaves in different scenarios, especially if you make trading decisions based on it. Furthermore, knowing the sensitivity of the price to various model parameters can have implications for calibration of the model, which can be a challenging procedure. Again we fix the benchmark set of parameters to be  $S_1 = 96$ ,  $S_2 = 100$ ,  $r = 0.1$ ,  $\delta_1 = 0.05$ ,  $\delta_2 = 0.05$ ,  $\sigma_1 = 0.5$ ,  $\sigma_2 = 1$ ,  $\rho = 0.5$ ,  $\rho_1 = 0.25$ ,  $\rho_2 = -0.5$ ,  $\sigma_v = 0.05$ ,  $v(0) = 0.04$ ,  $\kappa = 1.0$ ,  $\mu = 0.04$ ,  $T = 1$ . We also fix the FFT parameters as  $N = 256$ ,  $\bar{u}_{min} = 20$ , and  $\epsilon = (-3, 1)$ .

In figure 5 we look at how the price varies with the moneyness of the option and the strike price  $K$ . By fixing  $S_1(0) = 100$  and letting  $S_2(0)/S_1(0)$  vary from 70 to 120 we move from deep out-of-the-money to deep in-the-money options for different strike prices. The relationship shown by the figure is not surprising. The price increases with  $S_2(0)$  as the option becomes more in-the-money at the initial point in time, and naturally the price decreases with the strike price as it has opposite effect on the initial moneyness.

The next figure shows again how the price varies with the moneyness but this time along with the time to maturity  $T$ . In figure 6 we can see how the price increases with the time left to maturity although the effect seems to disappear as we move very deep out-of-the-money. The increase in the price with  $T$  also become less substantial as we move further into the future.

Figure 5: This figure illustrates how the spread option price changes due to variations in initial moneyness and strike price  $K$  while the rest of the parameters are fixed at the benchmark setting.



Moving on to the volatility scaling parameters of the underlying indexes, figure 7 illustrates how the price fluctuates with different values of  $\sigma_1$  and  $\sigma_2$ . The graph shows some interesting behavior. The spread option price is increasing non-linearly with both volatility scaling parameters in a symmetric way. But, if one of the parameters has a low value increasing the one currently being the lowest seems to lead to a decrease in the price until it hits roughly half the value of the larger one where the price starts to increase again. This means that an increase in the larger one or an equal increase in both always leads to an increase in the price. This relationship is explained by the positive correlation between the two assets. If we instead change the correlation between the assets from  $\rho = 0.5$  to  $\rho = -0.5$  the relationship changes, see figure 8. Now the price increases linearly with both parameters. This is reasonable considering that if the correlation is negative between the indexes an increase in either one of the volatility scaling parameters should be positive in the sense that it should increase the possibility of a larger spread between the indexes at maturity, which should be reflected in the price.

Now lets consider the correlation between the underlying indexes and the volatility process. In figure 9 we study the sensitivity to these parameters,  $\rho_1$  and

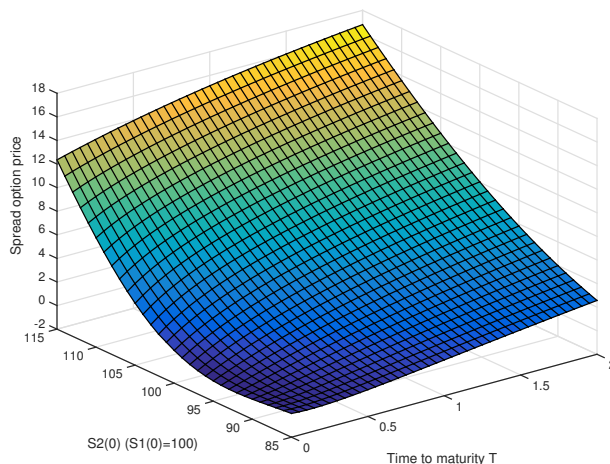


Figure 6: This figure shows how sensitive the spread option price is to variations in initial moneyness and time to maturity  $T$ . The rest of the parameters are fixed at the benchmark setting.

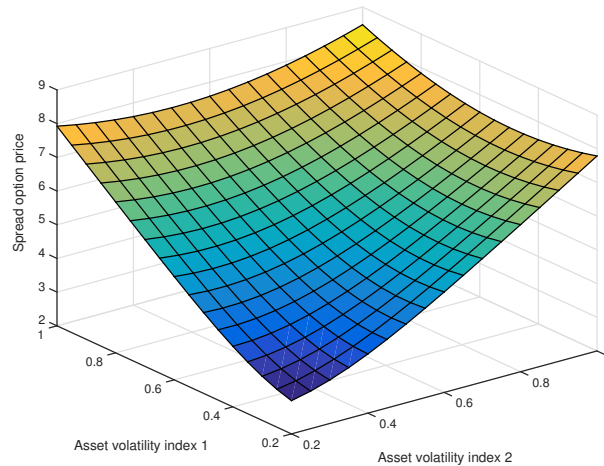
$\rho_2$ , while the other parameters are still part of the benchmark set. We see that increasing the correlation between the volatility process and index 2 gives higher prices, while the relationship is the opposite for the correlation between the volatility process and index 1. But, if we again change the correlation between the underlying indexes  $\rho$  from  $+0.5$  to  $-0.5$ , we see a positive relationship between the price and both  $\rho_1$  and  $\rho_2$ , see figure 10. However, judging from the graphs we see that these parameters have in fact very little impact on the price.

### 5.3 Stochastic Volatility and Jump Diffusion

#### 5.3.1 Accuracy & Speed

Following the same procedure as in the stochastic volatility case in the previous subsection we compare the prices produced by the FFT method to the benchmark prices in table 11. The benchmark prices are again produced by a Monte Carlo run with 1,000,000 simulations and 2,000 time steps. The following parameters are used:  $S_1 = 96$ ,  $S_2 = 100$ ,  $r = 0.1$ ,  $\delta_1 = 0.0$ ,  $\delta_2 = 0.0$ ,  $\sigma_1 = 0.5$ ,  $\sigma_2 = 1$ ,  $\rho = 0.5$ ,  $\rho_1 = 0.25$ ,  $\rho_2 = -0.5$ ,  $\rho_{Jumps} = \rho = 0.5$ ,  $\sigma_v = 0.05$ ,  $v(0) = 0.04$ ,  $\kappa = 1.0$ ,  $\mu = 0.04$ ,  $T = 1$ ,  $\lambda = 1.0$ ,  $z_1 = 0.05$ ,  $z_2 = 0.05$ ,  $q_1 = 0.05$ ,  $q_2 = 0.05$ . The integration interval is fixed at  $\bar{u}_{min} = 40$  and the damping coefficients are set as  $\epsilon = (-3, 1)$ . Inspecting the table we note that once more the FFT method produces accurate prices across all the strike prices investigated.

Figure 7: The spread option price increases with the volatility scaling parameters  $\sigma_1$  and  $\sigma_2$ . The non linear behavior is caused by the asset correlation  $\rho = 0.5$ .



In table 12 we study the computational speed for the FFT method under this model. It is shown that adding the random jumps to the model cost very little extra computational effort. The speed is again an average per option taken over 100 randomly generated options. Table 13 presents the computational speed for various Monte Carlo simulations and compares the estimated price to the FFT method and the benchmark. It is again obvious that to produce prices using simulation that are as accurate as those of the FFT method an enormous computational effort is required. Comparing to the model without jumps in the previous section we conclude that both the simulation time for the Monte Carlo method and the associated standard error has increased as a higher number of simulations is required for the method to converge when the jumps are added. This is in contrast to the FFT method where the computational time remains fairly constant.

In the next subsection we investigate the sensitivity to the choice of integration interval  $\bar{u}_{min}$  and the number of discretization points  $N$ .

Figure 8: The spread option price increases linearly with both volatility scaling parameters  $\sigma_1$  and  $\sigma_2$  when the asset correlation is changed to  $\rho = -0.5$ . The rest of the parameters are held constant at the benchmark setting.

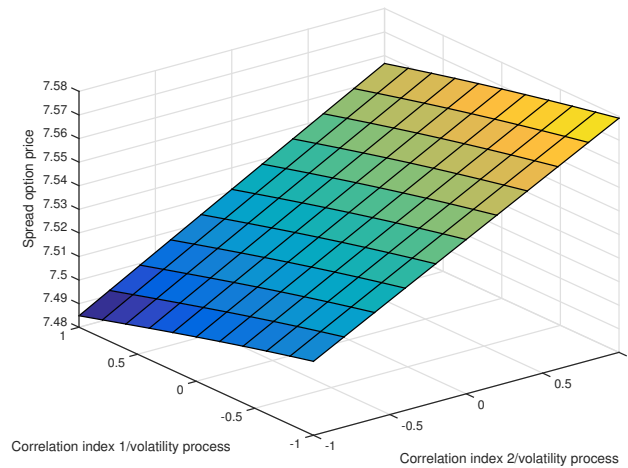
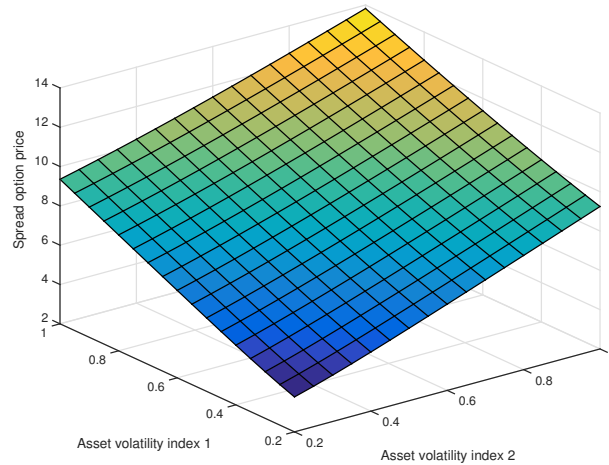
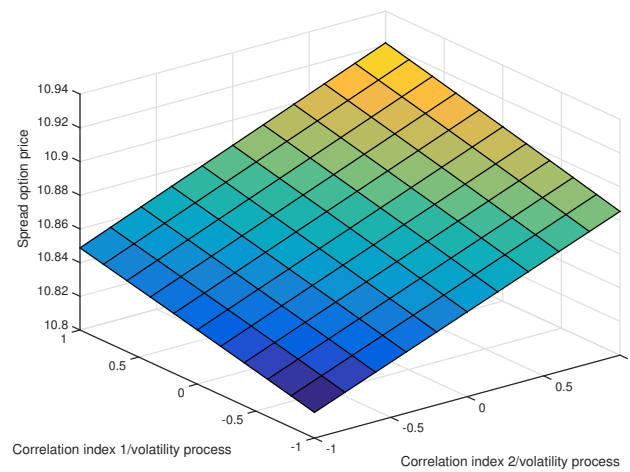


Figure 9: This figure shows how the spread option price changes with variations in the correlations between the volatility process and the underlying indexes  $\rho_1$  and  $\rho_2$ . The other parameters are fixed at benchmark setting (the asset correlation is  $\rho = 0.5$ ).

Figure 10: This figure shows how the spread option price changes with variations in the correlations between the volatility process and the underlying indexes  $\rho_1$  and  $\rho_2$  when the asset correlation is changed to  $\rho = -0.5$ .



Strike	MC Price	FFT					
	N=1e6, n=2000	N=128	N=256	N=512	N=1024	N=2048	
1	8.7602 (0.012)	5.89987783712154e-3	3.20540498631061e-4	3.20255606501618e-4	3.2025560668103e-4	3.2025560651050e-4	
1.5	8.5144 (0.012)	6.42344525857119e-3	6.02798880009914e-4	6.02488029660009e-4	6.0248802978968e-4	6.0248802980034e-4	
2	8.2733 (0.012)	6.41803349865988e-3	9.04706435729707e-4	9.04426858420848e-4	9.0442685858072e-4	9.0442685836933e-4	
2.5	8.0369 (0.012)	6.56593743391021e-3	1.200824396709880e-3	1.200558965910760e-3	1.20055896624116e-3	1.20055896607951e-3	
3	7.8052 (0.012)	7.22780914446997e-3	1.449592919169800e-3	1.449284135789600e-3	1.44928413582956e-3	1.44928413592993e-3	
3.5	7.5782 (0.012)	7.47700283106933e-3	1.712833809270010e-3	1.712525677519670e-3	1.71252567777014e-3	1.71252567781988e-3	
4	7.3557 (0.012)	7.37452896707946e-3	1.982204488410130e-3	1.981934141719320e-3	1.98193414193959e-3	1.98193414215009e-3	
4.5	7.1379 (0.011)	8.41260689821066e-3	2.299349879960390e-3	2.29900126559900e-3	2.29900126580063e-3	2.29900126584059e-3	
5	6.9247 (0.011)	9.29748076529968e-3	2.599570592630050e-3	2.599150753059830e-3	2.59915075316997e-3	2.59915075328987e-3	
5.5	6.7161 (0.011)	8.39037052224967e-3	2.890153709539160e-3	2.889870026479890e-3	2.88987002672947e-3	2.88987002676944e-3	
6	6.5120 (0.011)	8.82748227888985e-3	3.152483335939320e-3	3.152180430579850e-3	3.15218043078946e-3	3.15218043070953e-3	

Table 11: The table shows the actual errors of the FFT method compared to the benchmark prices under the stochastic volatility + jump diffusion model. The benchmark is calculated using a Monte Carlo method with 1,000,000 simulations and 2,000 time steps. The standard errors of the benchmark are given in parenthesis. The benchmark set of parameters is:  $S_1 = 96$ ,  $S_2 = 100$ ,  $r = 0.1$ ,  $\delta_1 = 0.0$ ,  $\delta_2 = 0.0$ ,  $\sigma_1 = 0.5$ ,  $\sigma_2 = 1$ ,  $\rho = 0.5$ ,  $\rho_1 = 0.25$ ,  $\rho_2 = -0.5$ ,  $\rho_{Jumps} = \rho = 0.5$ ,  $\sigma_v = 0.05$ ,  $v(0) = 0.04$ ,  $\kappa = 1.0$ ,  $\mu = 0.04$ ,  $T = 1$ ,  $\lambda = 1.0$ ,  $z_1 = 0.05$ ,  $z_2 = 0.05$ ,  $q_1 = 0.05$ ,  $q_2 = 0.05$  and  $\bar{u}_{min} = 40$ ,  $\epsilon = (-3, 1)$ .

Table 12: This table shows the average computational time in seconds for the FFT method under the stochastic volatility + jump diffusion model. The average is calculated over 100 randomly generated spread options. It is shown that adding the jumps to the model has very little impact on the computational speed.

Discretization	Comp. time (s)
N=128	0.058
N=265	0.199
N=512	0.825
N=1024	3.288
N=2048	12.63

Table 13: Computational speed along with an estimated price and its standard error for different Monte Carlo runs. The table shows that the FFT method produces a more accurate price in only a tiny fraction of the time. The price is calculated for  $K = 2$  under the benchmark set of parameters.

Time Steps	1000			2000			FFT N=128	Benchmark
Simulations	10000	50000	100000	10000	50000	100000	-	-
Comp. time (s)	123.33	616.23	1226.48	243.76	1226.95	2396.97	0.058	-
Price	8.3907	8.2641	8.2611	8.3589	8.3375	8.2972	8.2738	8.2733
SE	0.1218	0.0544	0.0382	0.1231	0.0542	0.0381	-	0.0121

### 5.3.2 Sensitivity to the Discretization Parameters

To analyze the sensitivity to the truncation and discretization parameters under the third model we follow the same procedure as in the stochastic volatility case. 19 options under with different strike prices are used to evaluate the impact of the parameters  $N$  and  $\bar{u}_{min}$  on the accuracy of the method. The parameters are:  $S_1 = 100$ ,  $S_2 = 110$ ,  $r = 0.1$ ,  $\delta_1 = 0.0$ ,  $\delta_2 = 0.0$ ,  $\sigma_1 = 0.5$ ,  $\sigma_2 = 1$ ,  $\rho = 0.5$ ,  $\rho_1 = 0.25$ ,  $\rho_2 = -0.5$ ,  $\rho_{Jumps} = \rho = 0.5$ ,  $\sigma_v = 0.05$ ,  $v(0) = 0.04$ ,  $\kappa = 1.0$ ,  $\mu = 0.04$ ,  $T = 1$ ,  $\lambda = 1.0$ ,  $z_1 = 0.05$ ,  $z_2 = 0.05$ ,  $q_1 = 0.05$ ,  $q_2 = 0.05$  and  $K = 2, 3, 4, \dots, 20$ . Looking at the results in table 14 and figure 11 we see a similar behavior as in the two previous market models, although one thing stands out. It seems that, starting from the smallest integration interval ( $\bar{u}_{min} = 20$ ), we can again reduce the error marginally by increasing  $N$ , but even at the finest grids the gain from increasing the minimum integration interval  $\bar{u}_{min}$  represented by a lower truncation error does not weigh up the associated loss resulting from the larger discretization error. The analysis suggests that under the model with stochastic volatility and random jumps the optimal choice is to set the integration interval at  $\bar{u}_{min} = 20$ , irrespective of our choice of



discretization parameter  $N$ . Furthermore, we note that again the errors are bigger in magnitude than in the previous model, this could possibly be explained by the accuracy of the benchmark itself. The added jumps causes the Monte Carlo simulation to converge even slower leading to a higher uncertainty in the benchmark prices. Though it could also be inherent in the FFT method caused by a more complex joint characteristic function.

Table 14: Mean absolute relative error (MAPE) for different choices of  $\bar{u}_{min}$  and discretization  $N$  for the SV + Jump diffusion model. The MAPE is calculated based on 19 options of different moneyness.

<b>u_min</b>	<b>N</b>			
	<b>128</b>	<b>256</b>	<b>512</b>	<b>1024</b>
<b>20</b>	2.1636e-3	2.1633e-3	2.1633e-3	2.1633e-3
<b>40</b>	4.1742e-3	2.1671e-3	2.1670e-3	2.1670e-3
<b>60</b>	-	2.2529e-3	2.1670e-3	2.1670e-3
<b>80</b>	-	4.1742e-3	2.1671e-3	2.1670e-3
<b>100</b>	-	-	2.1739e-3	2.1670e-3
<b>120</b>	-	-	2.2529e-3	2.1670e-3
<b>140</b>	-	-	2.6185e-3	2.1670e-3
<b>160</b>	-	-	3.9677e-3	2.1671e-3
<b>200</b>	-	-	-	2.1730e-3
<b>240</b>	-	-	-	3.7715e-3
<b>280</b>	-	-	-	3.9756e-3

### 5.3.3 Sensitivity to the Damping Parameters

The mean absolute relative error is again calculated using the 19 options with different strike prices under the benchmark set of parameters for different choices of damping parameters  $\epsilon = (\epsilon_1, \epsilon_2)$ . The sensitivity to the damping parameters seems unchanged by adding the jumps to the stochastic volatility model. Studying the results in table 15 we see that we want to impose the same restrictions on the parameters as in the previous case to avoid hurting the accuracy of the method, that is  $\epsilon_2 \geq 0.8$  and  $\epsilon_1 + \epsilon_2 \leq -1.6$ . The error function is again illustrated graphically in figure 12.

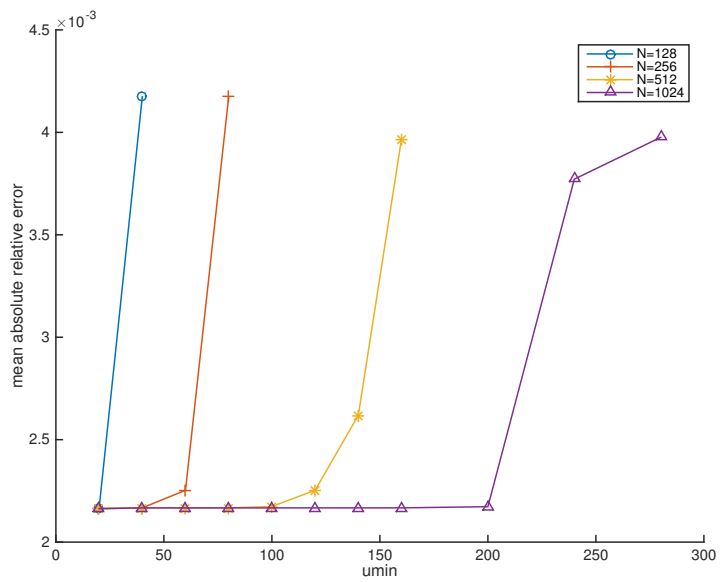
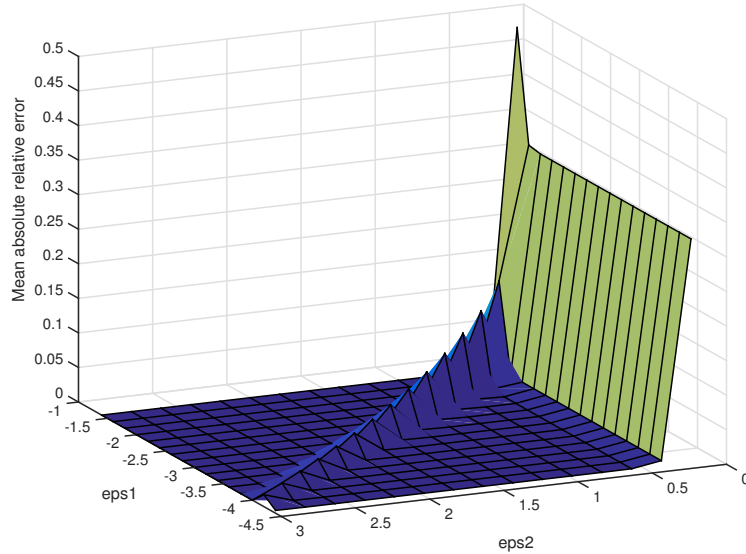


Figure 11: Mean absolute relative error (MAPE) for different choices of  $\bar{u}_{min}$  and discretization  $N$  under the stochastic volatility + jumps model. The MAPE is calculated based on 19 options of different moneyness.

Table 15: This table shows the mean absolute relative error (MAPE) for different choices of damping parameters  $\epsilon = (\epsilon_1, \epsilon_2)$  under the stochastic volatility + jump diffusion market model. The MAPE is calculated based on 19 options of different moneyness.

$\epsilon_2/\epsilon_1$	-4.4	-4.2	-4.0	-3.8	-3.6	-3.4	-3.2	-3.0	-2.8	-2.6	-2.4	-2.2	-2.0	-1.8	-1.6	-1.4
<b>0.2</b>	0.33	0.33	0.33	0.33	0.33	0.33	0.33	0.33	0.33	0.33	0.33	0.33	0.33	0.33	0.33	0.49
<b>0.4</b>	1.06e-2	1.06e-2	1.06e-2	1.06e-2	1.06e-2	1.06e-2	1.06e-2	1.06e-2	1.06e-2	1.06e-2	1.06e-2	1.06e-2	1.06e-2	1.30e-2	0.14	-
<b>0.6</b>	3.88e-3	3.88e-3	3.88e-3	3.88e-3	3.88e-3	3.88e-3	3.88e-3	3.88e-3	3.88e-3	3.88e-3	3.89e-3	3.93e-3	5.86e-3	0.11	-	-
<b>0.8</b>	3.72e-3	3.72e-3	3.71e-3	3.71e-3	3.71e-3	3.71e-3	3.71e-3	3.71e-3	3.71e-3	3.72e-3	3.75e-3	5.38e-3	9.15e-2	-	-	-
<b>1.0</b>	3.71e-3	3.71e-3	3.71e-3	3.71e-3	3.71e-3	3.71e-3	3.71e-3	3.71e-3	3.71e-3	3.74e-3	5.12e-3	7.68e-2	-	-	-	-
<b>1.2</b>	3.71e-3	3.71e-3	3.71e-3	3.71e-3	3.71e-3	3.71e-3	3.71e-3	3.71e-3	3.73e-3	4.89e-3	6.45e-2	-	-	-	-	-
<b>1.4</b>	3.71e-3	3.71e-3	3.71e-3	3.71e-3	3.71e-3	3.71e-3	3.71e-3	3.73e-3	4.71e-3	5.42e-2	-	-	-	-	-	-
<b>1.6</b>	3.71e-3	3.71e-3	3.71e-3	3.71e-3	3.71e-3	3.71e-3	3.73e-3	4.55e-3	4.56e-2	-	-	-	-	-	-	-
<b>1.8</b>	3.71e-3	3.71e-3	3.71e-3	3.71e-3	3.71e-3	3.72e-3	4.42e-3	3.92e-2	-	-	-	-	-	-	-	-
<b>2.0</b>	3.71e-3	3.71e-3	3.71e-3	3.71e-3	3.72e-3	4.32e-3	3.39e-2	-	-	-	-	-	-	-	-	-
<b>2.2</b>	3.71e-3	3.71e-3	3.71e-3	3.72e-3	4.22e-3	2.93e-2	-	-	-	-	-	-	-	-	-	-
<b>2.4</b>	3.71e-3	3.71e-3	3.72e-3	4.15e-3	2.55e-2	-	-	-	-	-	-	-	-	-	-	-
<b>2.6</b>	3.71e-3	3.72e-3	4.08e-3	2.23e-2	-	-	-	-	-	-	-	-	-	-	-	-
<b>2.8</b>	3.72e-3	4.03e-3	1.96e-2	-	-	-	-	-	-	-	-	-	-	-	-	-
<b>3.0</b>	3.99e-3	1.73e-2	-	-	-	-	-	-	-	-	-	-	-	-	-	-

Figure 12: Mean absolute relative error (MAPE) for different choices of damping parameters  $\epsilon = (\epsilon_1, \epsilon_2)$  under the stochastic volatility model illustrated graphically. The MAPE is calculated based on 19 options.



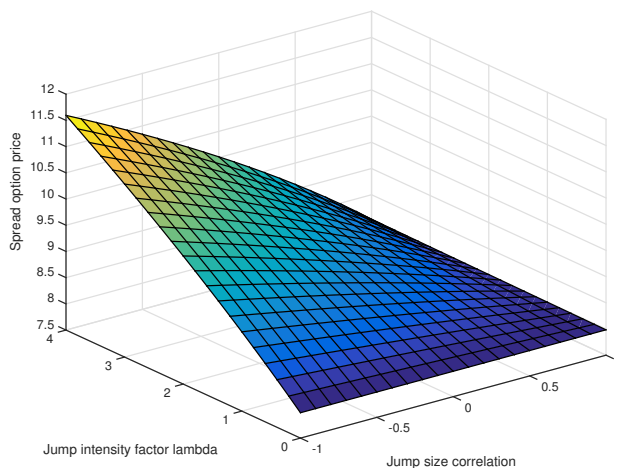
### 5.3.4 Price Sensitivity to Market Parameters

Lastly we study the sensitivity of the price to the market parameters introduced by adding the random jumps to the model. The parameters are fixed according to the original benchmark set, although the jump size correlation is set to zero to easier visualize the effects of each component. The parameters are:  $S_1 = 96$ ,  $S_2 = 100$ ,  $r = 0.1$ ,  $\delta_1 = 0.0$ ,  $\delta_2 = 0.0$ ,  $\sigma_1 = 0.5$ ,  $\sigma_2 = 1$ ,  $\rho = 0.5$ ,  $\rho_1 = 0.25$ ,  $\rho_2 = -0.5$ ,  $\rho_{Jumps} = 0$ ,  $\sigma_v = 0.05$ ,  $v(0) = 0.04$ ,  $\kappa = 1.0$ ,  $\mu = 0.04$ ,  $T = 1$ ,  $\lambda = 1.0$ ,  $z_1 = 0.05$ ,  $z_2 = 0.05$ ,  $q_1 = 0.05$ ,  $q_2 = 0.05$ ,  $K = 2$ . Furthermore, the model parameters are fixed at  $N = 256$ ,  $\bar{u}_{min} = 20$  and  $\epsilon = (-3, 1)$ . We now analyze how variations in the jump diffusion parameters  $\lambda, z_i, q_i$  and  $\rho_{Jumps}$  affect the price of the spread option.

In figure 13 we study the impact of the the jump intensity factor  $\lambda$  and the jump size correlation coefficient  $\rho_{Jumps}$ . It is clear that generally a higher jump intensity implies a higher spread option price. This is not surprising considering that a higher number of jumps results in a greater probability of a larger widening of the spread before the option matures. This is true except for the case when  $\rho_{Jumps} = 1$ . If the correlation between the jump sizes is exactly one, the jumps will not have any effect on the difference between the indexes

(remembering that the jump sizes are equal) and thus an increase in the intensity of the jumps will not matter either. Additionally, the price is decreasing with the jump correlation and therefore has its maximum value when  $\rho_{Jumps} = -1$  along with a high jump intensity factor, this is not surprising, since if the indexes jump in opposite directions the spread naturally increases.

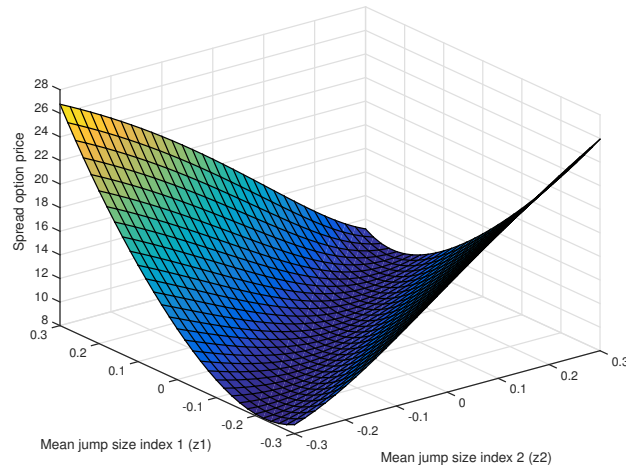
Figure 13: This figure shows how the spread option price varies with the value of the jump intensity factor  $\lambda$  and the jump size correlation  $\rho_{Jumps}$  while the rest of the parameters are fixed at the benchmark setting. The price is an increasing function of the jump intensity factor and a decreasing function of the jump size correlation.



Next we consider variations in the parameters governing the jump sizes. Figure 14 shows how the price is affected when varying the mean jump size parameters,  $z_1$  and  $z_2$ . The graph is quite interesting and show that there is a high sensitivity in the price towards the jump size parameters. Firstly, the plot suggest that the price is the highest when  $z_1$  and  $z_2$  are of opposite signs. This is intuitively what we would expect, since jumps in different directions will clearly lead to a greater widening of the spread, this is analogous with the jump size correlation being negative. Secondly, the graph has its lowest point around where the jump sizes are equal, which also is reasonable considering that if we expect the indexes to jump equally this will not have an affect on the difference between them. Importantly, the analysis points out that the price is very sensitive to these parameters, meaning that a small change can have a significant impact on the price.

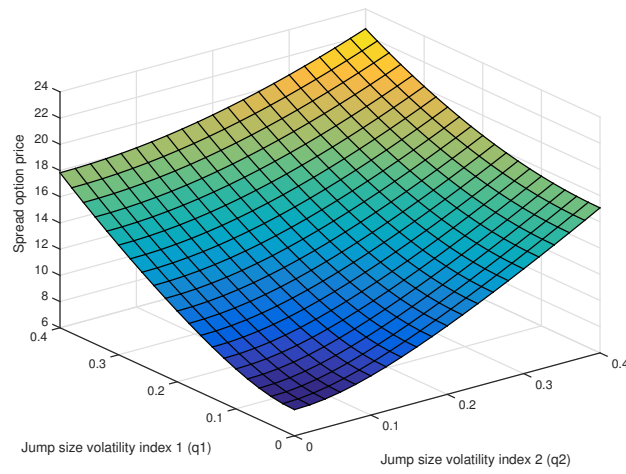
Lastly we look at the impact of the jump size volatility parameters  $q_1$  and  $q_2$  in figure 15. The graph illustrates that the spread option price increases non-linearly with both jump size volatility parameters. Much like the jump size

Figure 14: Variations in the mean jump size parameters can have a significant impact on the spread option price. The figure shows the price for different values of  $z_1$  and  $z_2$  while the rest of the parameters are held fixed at the benchmark setting.



parameters, these parameters are also having a big impact on the option price, revealing a high sensitivity.

Figure 15: This figure shows the price sensitivity to changes in the jump size volatility parameters,  $q_1$  and  $q_2$ . The other parameters are fixed at the benchmark setting. The figure reveals a high sensitivity to jump size volatility parameters.



## 6 Conclusions

In this thesis we have investigated the pricing of spread options using the fast Fourier transform. By implementing the FFT method proposed by Hurd and Zhou under three different market models we have successfully extended the work of Dempster and Hong [7] and Hurd and Zhou [10] to include random jumps in the asset dynamics. We have analyzed the performance of the model under the 2-asset geometric Brownian motion framework, the stochastic volatility model and the stochastic volatility model including jumps. Under the first model it was shown that the method produces very accurate prices, beating all the other methods that was explored. However, it was not as computationally fast as some of the closed form analytical approximations, presenting a trade off between accuracy and speed. The real strength of the FFT method was demonstrated when a stochastic volatility structure was introduced. By adding this factor the computational effort required by Monte Carlo methods increases dramatically. Meanwhile, adding complexity to the market model only amounts to changing the joint characteristic function in the Fourier methods, which implies a very small extra computational cost. We showed that our FFT method produces accurate prices under the stochastic volatility model in only a tiny fraction of the time it takes to reach a price by simulation. Adding random jumps to the model puts even more strain on the Monte Carlo methods as the jumps causes the method to converge even slower.

In addition to evaluating the FFT method under the different market models we have analyzed the sensitivity to the parameters inherent in the method that need to be specified. We provide valuable information regarding specification of both the integration interval and the damping parameters under all models. From the results of the experiments we make clear suggestions concerning how to choose these parameters. Although the method is found to be robust to changes in these parameters there are pitfalls one should be aware of when implementing it.

Furthermore, we investigate the spread option price sensitivity to the various market parameters arising from the stochastic volatility structure and the random jump process. This provides great insight into the behavior of the model, which certainly can be useful when making trading decisions based on it. We show that the price is very sensitive to changes in the parameters introduced by the jump diffusion. This means that the model is flexible and can be tuned to a diverse set of characteristics present in data from the financial markets. This flexibility allows us to calibrate the model to explain different sort of behaviors arising in the complex reality. However, the calibration of the model is a whole other problem and can be a challenging statistical procedure, although a sensitivity analysis like ours can provide useful information when dealing with this problem.



## References

- [1] DS Bates. Jumps and stochastic volatility: exchange rate processes implicit in deutsche mark options. *Review of Financial Studies*, 9(1):69–107, 1996.
- [2] T. Björk. *Arbitrage Theory in Continuous Time*. Oxford Finance Series. OUP Oxford, 2009.
- [3] René Carmona and Valdo Durrleman. Pricing and hedging spread options. *SIAM Review*, pages 627–685, 2003.
- [4] Peter Carr and Dilip B. Madan. Option valuation using the fast fourier transform. *Journal of computational finance*, 2:61–73, 1999.
- [5] James W. Cooley and John W. Tukey. An algorithm for the machine calculation of complex fourier series. *Mathematics of Computation*, pages 297–301, 1965.
- [6] John C Cox, Ingersoll Jonathan E, and Stephen A Ross. A theory of the term structure of interest rates. *Econometrica*, 53(2):385–407, 1985.
- [7] M.A.H. Dempster and S. S. G. Hong. Spread option valuation and the fast fourier transform. Technical report, In proceedings of the international conference on computational finance and its applications (ICCF), 2000.
- [8] Paul Godfrey. A note on the computation of the convergent lanczos complex gamma approximation. 2001.
- [9] Steven L. Heston. A closed-form solution for options with stochastic volatility with applications to bond and currency options. *Review of Financial Studies*, 6:327–343, 1993.
- [10] Thomas R. Hurd and Zhuowei Zhou. A fourier transform method for spread option pricing. *SIAM J. Financial Math.*, 1(1):142–157, 2010.
- [11] E. Kirk. Correlations in the energy markets. *Managing Energy Price Risk, Risk Publications and Enron, London*, pages 71–78, 1995.
- [12] E. Lindström, H. Madsen, and J.N. Nielsen. *Statistics for Finance*. Chapman & Hall/CRC Texts in Statistical Science. Taylor & Francis, 2015.
- [13] S. Deng M. Li and J. Zhou. Closed-form approximations for spread option prices and greeks. *J. Derivatives*, 15(3):58–80, 2008.
- [14] William Margrabe. The value of an option to exchange one asset for another. *The Journal of Finance*, 33(1):177–186, 1978.
- [15] Robert C. Merton. Paul samuelson and financial economics. *American Economist*, 50(2):262–300, 2006.
- [16] P. Olivares and M. Cane. Pricing Spread Options under Stochastic Correlation and Jump-Diffusion Models. *ArXiv e-prints*, September 2014.

- [17] Brad Osgood. *The Fourier Transform and Its Applications*. 2007. Electrical Engineering Department. Stanford University.
- [18] Martin Sköld. Computer intensive statistical methods, lecture notes for fms091/mas221. *2nd print, Lund University*, 2006.
- [19] M. Suárez-Taboada and C. Vázquez. A numerical method for pricing spread options on libor rates with a pde model. *Mathematical and Computer Modelling*, 52(78):1074 – 1080, 2010. Mathematical Models in Medicine, Business and Engineering 2009.
- [20] L. Trigeorgis. *Real Options: Managerial Flexibility and Strategy in Resource Allocation*. MIT Press, 1996.
- [21] Aanand Venkatramanan and Carol Alexander. Closed form approximations for spread options. *Applied Mathematical Finance*, 18(5):447–472, 2011.